Technische Universität München

Urban Liner Aircraft Concept

Team

Christian Decher

Daniel Metzler

Soma Varga

Academic Support and Advisors

Institute of Aircraft Design, TU Munich

Prof. Dr. Mirko Hornung

Lysandros Anastasopoulos

Submitted on June 30th, 2017

Lehrstuhl für Luftfahrtsysteme

Team Members

Christian Decher, BSc., *Team Lead*

Master student in Aerospace Engineering and Engineering&Management, 3rd semester

Focus on Propulsion System

Daniel Metzler, BSc.

Master student in Aerospace Engineering, 2nd semester

Focus on CAD and Structures

Soma Varga, BSc.

Master student in Aerospace Engineering, 2nd semester

Focus on Aerodynamics

Technische Universität München

Technische Universität München . Lehrstuhl für Luftfahrtsysteme
Boltzmannstraße 15 . 85748 Garching . Germany
Lehrstuhl für Luftfahrtsysteme
Institut für Luft- und Raumfahrt
Boltzmannstraße 15
85748 Garching b. München

Fakultät für Maschinenwesen
Institut für Luft- & Raumfahrt
Lehrstuhl für Luftfahrtsysteme

Prof. Dr.-Ing.
Mirko Hornung

Boltzmannstraße 15
85748 Garching bei München

Tel +49.89.289.15981
Fax +49.89.289.15982

sekretariat@lls.mw.tum.de
www.lls.mw.tum.de

Garching, 23. Juni 2017

Bestätigungsschreiben

Sehr geehrte Damen und Herren,

mit diesem Schreiben wird bescheinigt, dass der Beitrag der Studierenden zum studentischen Wettbewerb *DLR-NASA-Challenge 2017* (Kategorie 2: effizientes Transportflugzeug) am Lehrstuhl für Luftfahrtsysteme geprüft und genehmigt wurde. Die Einreichung des Berichts wird damit befürwortet.

Bei weiteren Fragen können Sie sich gerne an mich oder den betreuenden Mitarbeiter Herrn Lysandros Anastasopoulos (lysandros.anastasopoulos@tum.de) wenden.

Mit freundlichen Grüßen

Univ. Prof. Dr.-Ing. Mirko Hornung
Ordinarius des Lehrstuhls für Luftfahrtsysteme

Technische Universität München

Technische Universität München . Lehrstuhl für Luftfahrtsysteme
Boltzmannstraße 15 . 85748 Garching . Germany
Lehrstuhl für Luftfahrtsysteme
Institut für Luft- und Raumfahrt
Boltzmannstraße 15
85748 Garching b. München

Fakultät für Maschinenwesen
Institut für Luft- & Raumfahrt
Lehrstuhl für Luftfahrtsysteme

Boltzmannstraße 15
85748 Garching bei München

Tel +49.89.289.15981
Fax +49.89.289.15982

sekretariat@lls.mw.tum.de
www.lls.mw.tum.de

Garching, 29. Juni 2017

Bestätigungsschreiben

Sehr geehrte Damen und Herren,

hiermit bestätige ich, dass die Mitglieder der studentischen Arbeitsgruppe für die Kategorie 2, effizientes Transportflugzeug:

- Christian Decher
- Daniel Metzler
- Soma Varga

die Arbeit zum Wettbewerb *DLR-NASA-Challenge 2017* eigenständig angerfertigt haben. Bei Fragen stehe ich Ihnen jederzeit zur Verfügung.

Mit freundlichen Grüßen
Lysandros Anastasopoulos

Betreuender wissenschaftlicher Mitarbeiter

Anastasopoulos L.

M.Sc. Lysandros Anastasopoulos

Technische Universität München
Fakultät für Maschinenwesen
Lehrstuhl für Luftfahrtsysteme

Boltzmannstraße 15
85748 Garching
Tel + 49.89.289.15796
Fax + 49.89.289.15982
lysandros.anastasopoulos@tum.de
www.lls.mw.tum.de

Abstract

For future air traffic to remain competitive in a rapidly changing transportation market, sustainable growth has to be achieved through significant improvements in aircraft efficiency and emissions. These are unlikely to be realized through the incremental improvements of existing aircraft configurations. Therefore alternative propulsion systems and their integration into novel aircraft designs may become key enablers for future air transport solutions.

Within the scope of the 2017 DLR and NASA Design Challenge an interdisciplinary design study was conducted to assess and evaluate possible aircraft configurations which enable the integration of alternative propulsion technologies. Major attention was given to the simulation and assessment of key aircraft features including the airframe, aerodynamics and propulsion system. The resulting Urban Liner design incorporates and combines advantages of promising aerospace technologies to achieve the ambitious goals of DLR and NASA and deliver outstanding operational performance.

In this report design considerations and technical developments are discussed and simulation results are presented. A market analysis identifies future trends and demands in aviation, deriving a targeted market positioning with respect to the technical capabilities of hybrid propulsion. The resulting operational requirements dictate the concept's initial sizing and performance figures. The Urban Liner's basic layout integrates noise reduction objectives at the initial design stage to maximize potential savings. The resulting low noise configuration is iteratively optimized from an aerodynamic and structural standpoint to integrate the alternative propulsion design.

To identify an engine technology that best fits this silent configuration and drastically reduces nitrogen oxide emissions, promising propulsion technologies are assessed and a final design is selected from a multivariable GasTurb design optimization study. It is established that a hybrid propulsion system enables the usage of a single turbo fan, provided that the specific energy densities of batteries is above a critical limit of 600 Wh/kg. The resulting single turbofan hybrid configuration has the potential to reduce LTO and cruise NO_x emissions by more than 80%.

To compensate the additional system weight a concept for a combinational use of the electric fans is presented. The final design includes a split wing root structure which encapsulates the aircraft cabin and a system for maintaining laminar flow during cruise. In a 300 PAX configuration the U-Liner offers a 53% improvement in fuel consumption per PAX relative to a current generation Airbus A321.

Contents

List of Figures

List of Tables

Nomenclature

ACARE Advisory Council for Aviation Research and Innovation in Europe

ALI Attachment Line Instability

AR Aspect Ratio

BPR Bypass Ratio

BWB Blended Wing Body

CAEP Committee on Aviation Environmental Protection

CCW Circulation Control Wing

CeRAS Central Reference Aircraft Data System Specifications

CESTOL Cruise Efficient Short Take Off and Landing

CFD Computational Fluid Dynamics

CFI Cross-Flow Instability

CG Center of Gravity

COC Cash Operating Costs

CS Certification Specifications

DLR German Aerospace Center

DOC Direct Operating Costs

EASA European Aviation Safety Agency

EF Electric Fan

EIS Entry into Service

EPNdB Effective Perceived Noise Level

ETOPS Extanded Range Operations

FAA Federal Aviation Administration

FEM Finite Element Methods

Fig Figure

FL Flight Level

GTF Geared Turbofan

HLFC Hybrid Laminar Flow Control

HPT High Pressure Turbine

ICA Initial Cruise Altitude

ICAO International Civil Aviation Organization

IRA Intercooled Recuperated Aero Engine

ISA International Standard Atmosphere

L/D Lift over Drag Ratio

LE Leading Edge

LTO Landing and Take Off

Ma Mach number

MIT Massachusetts Institute of Technology

MTOW Maximum Take Off Weight

NASA National Aeronautics and Space Administration

NEWAC New Environmentally Friendly Aero Engine Core Concepts

NLF Natural Laminar Flow

NOx Nitrogen Oxide

OASPL Overall Sound Pressure Level

OEI One Engine Inoperative

OEW Operational Empty Weight

ONERA French National Research Center

OPR Overall Pressure Ratio

PAX Passenger

Re Reynolds Number

ROC Rate of Climb

RPK Revenue Passenger Kilometer

RQL Rich Burn Quick Mix Lean Burn

SEP Specific Excess Power

SM Static Margin

TE Trailing Edge

TeDP Turbo Electric Distributed Propulsion System

TET Turbine Entrance Temperature

TF Turbo Fan

TOC Top of Climb

TRL Technology Readiness Level

TSFC Thrust Specific Fuel Consumption

TSI Tollmien-Schlichting Instability

1 Introduction

Global air traffic growth at its current pace can only be sustainable if environmental and societal needs are actively considered during development of new aircraft. In order to achieve the goals defined by the Euorpean Commission in Flightpath 2050, ACARE and NASA, new aircraft concepts must be developed and implemented as current configurations are unlikely to meet these goals [1]. Urbanization and emerging city-pairs play a significant role as they entail high-frequency passenger and freight transport demand between major hubs as well as smaller city airports. Connecting major hubs already accounts for a majority of todays air traffic [2] and due to the continuous growth prediction of metropol cities, especially in the Asian Pacific area, the need for high-capacity aircraft will continuously grow. This market segment consequently yields enormous economic potential for future airline operations [3].

The challenge of reducing aircraft fuel consumption, pollutant and noise emissions while maintaining the industry's exceptionally high safety standards relies on the conscientious application of new technologies including fully or hybrid electric propulsion systems. Increasing environmental awareness of the aerospace industry also resulted in the introduction of NOx limtations to the ICAO regulations on aircraft emission. The initial target of improving local air quality around airports was eventually expanded to other flight phases after additional concerns were raised about the NOx emissions produced during cruise [4]. To this point commercial aircraft design was primarily focused on minimizing operating costs while environmental concerns were brought up at a post design stage [5]. In order to achieve outstanding environmental performance during takeoff and landing as well as in cruise, environmental considerations must be integrated at an early stage of the aircraft design process. Hence for future air transport to be able to compete with new forms of transportation especially on short distances it must decrease its dependence on oil as the industry is vulnerable to fuel prices [4].

The aim of this project is to address these societal and technological changes by developing an ultra-efficient low-noise subsonic aircraft with an entry into service (EIS) horizon of 2035, bearing in mind the associated challenges such as low operating costs and passenger acceptance. This implies fast turnaround times for airlines whereas passengers are interested in comfort and quick boarding, among other things.

Based on a market analysis and industry forecasts, the requirements for such an aircraft are presented in the following section. The decisions leading to the Urban Liner Concept are outlined as a result of the market requirements. With an EIS in 2035, different scenarios are conceivable regarding the market evolution but also technological developments. Designing a future aircraft fulfilling the goals set by international organisations thus implies diverse assumptions relating to regulatory constraints. For the sake of concept feasibility, a minimum technological readiness level of 5 is suggested. The aircraft architecture therefore rests on previous research by DLR and NASA in combination with relevant scientific work. Detailed descriptions of the integrated systems and enabling technologies are provided to foster the understanding of the concept at hand. The focus of this paper is directed on the overall aircraft design and implies current technologies such as chevron nozzles without explicit indication.

The U-Liner incorporates a wide variety of technological advancements with the focus on combining these into an overall feasible and consistent aircraft configuration. The hybrid propulsion configuration in conjunction with laminar flow control and advanced composite materials provides new perspectives on component arrangement possibilities. As the propulsion system represents a major enabler of the overall design, a significant part is dedicated towards its specifications.

Progress in fields such as battery technology, material science and production engineering opens several new possibilities but can also limit the applicability of concept studies. In order to prove the concept to be viable, a sensitivity analysis follows the aircraft system description. Finally an overview is provided to assess the Urban Liner Concept based on the societal and environmental requirements.

2 Meeting Future Demands

Resulting from the EIS horizon of 2035, the aircraft will need to address the market until at least 2050. As these forecasts are extremely vague, the necessary possibility of adapting to new market segments influences the overall design. The strong increase in RPKs predicts 41'030 new deliveries within the next two decades [6]. A big part thereof results from Asia's economic growth, followed by North America and Europe [6]. Deriving these global trends, demand for cruise-efficient short takeoff and landing (CESTOL) jet aircraft emerges to fulfill environmental goals on one hand and provide market fit on the other. The specification for seating at least 200 passengers puts the U-Liner in the range of current twin-aisle aircraft.

Low-cost carriers will potentially control about 60% of the short-haul market [3], asking for fast turnaround times and high passenger densities. Given that the average stage-length of current commercial air transport is relatively short (3668nm for an A330-200 [7]) only medium range capabilities are required. A minimum range of 6000km however is regarded as essential for flexible route planning which also coincides with the 5950km target design range of the Airbus A321 [8]. This represents a reasonable range for hybrid electric propulsion.

The demand for aircraft ultimately stems from airline operations, favoring low operating costs and operational freedom. In combination with increasing air traffic, this opens up a scenario of twin-aisle aircraft entering the single-aisle market on short-haul flights assuming the operating costs thereof are within comparable reach for hybrid powered aircraft. Passenger densities for these twin-aisle airplanes can be lowered and therefore quicker turnaround times become possible as the PAX per aisle ratio decreases.

Next to commercial air transport, freight traffic is expected to grow even faster than passenger traffic at 4.8% per year with the biggest opportunities in mid-sized freighters [3]. About 63% of freighter deliveries will be met by converted passenger airplanes [6].

The combination of these market constraints suggests a medium range aircraft in the 270-300 passenger spectrum with sufficient payload capabilities to serve as a freighter as well. In order to best adapt to the market situation 20 years from EIS, the option of a family concept shall be maintained. An eye should also be kept on production costs and times as the worldwide twin-aisle fleet will more than double until 2032 [3]. This strengthens the idea of family building because both production costs and times entail a fairly simple fuselage design with recurring construction patterns. Furthermore the engineering experience available in designing tube-like fuselages significantly reduces development costs.

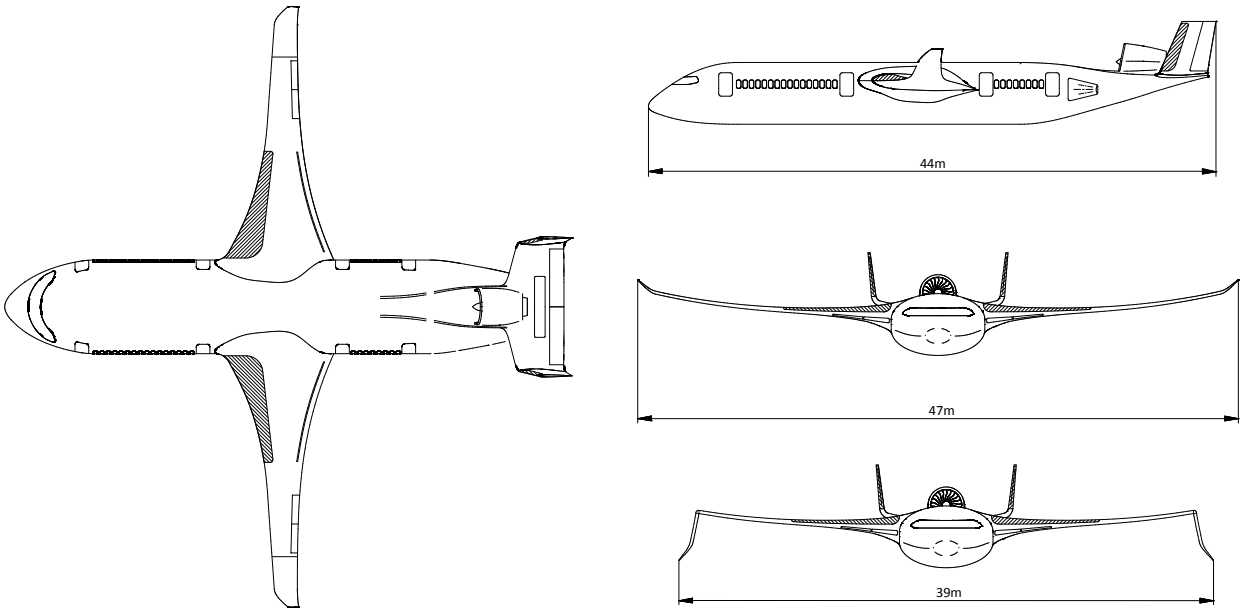

Figure 1: Three-View Drawing of the Urban Liner Concept

The goal of reaching ultimate operational freedom includes fitting into either a 36m airport box with precision parking assistance systems or a 39m box. The latter is presumed to be a consequence of progressively larger aircraft being demanded by the continues growth in air traffic [3]. As soon as airlines are able to operate twin-aisle aircraft equally to single-aisle aircraft at airports regarding costs and space, the blurring of single- and twin-aisle market segments is predestined. This fosters once more the demand for high seat capacity on the baseline aircraft. Folding wingtips offer the possibility to increase the maximum wing span with regard to the parking position, however not to the extent required for the specified lift generation capability. Therefore the fuselage is designed as a lifting widebody which helps in generating lift.

In order to meet the market requirement of 300 passengers in a single-class configuration, the U-Liner's twin-aisle cabin is equipped with eleven seats abreast. The widebody optionally allows for faster turnaround times through a triple-aisle cabin configuration with ten seats abreast in which case the U-Liner can seat up to 272 passengers.

Future demand for low separation distances at airports restrict the maximum takeoff weight to remain below 136t to minimize wake turbulence and thereby takeoff intervals. Combined with the payload requirement, the upper limit of 136t was chosen.

As a result of the wide fuselage and the MTOW specification, the U-Liner is capable of transporting up to 26 LD3 cargo containers on the lower deck, a part of which are used as battery containers to power the hybrid propulsion system. This puts the aircraft in direct comparison with the A330-200 (26 LD3s [8]) despite the U-Liner's shorter cabin length.

The propulsion system is designed to meet the environmental requirements regarding noise emissions, fuel consumption and LTO NOx as well as cruise NOx emissions. Given that today's aircraft will still hold a major share of the worldwide fleet in 2035, minimum cruise speeds of Ma 0.75 are also necessary for conveniently integrating the U-Liner into air traffic.

3 Low Noise Design

For the U-Liners 2035 entry into service horizon, the goal is to reduce noise emissions by at least 42dB relative to ICAO Stage 4, resulting in a maximum cumulative effective perceived noise level of 249.6 EPNdB for the specified MTOW. As the broad range of human noise perception is characterized by a logarithmic scale of sound pressure levels, not only technology needs to improve drastically [1] but also regulations need to adapt in favor of these novel technologies.

Sound pressure levels are measured at the sideline, approach and flyover which emphasizes the importance of a silent overall aircraft configuration rather than single technology improvements. At the approach, airframe noise and engine noise are roughly the same size [9] whereas fan noise dominates flyover and sideline noise levels [10]. Airframe noise is mainly caused by the landing gear and wing high-lift devices [1, 9] and scales predominantly with airspeed and distance to the observer [11]. This emphasizes the importance of low approach speeds through high lift coefficients, optimized approach procedures and improved climb rates.

Engine noise primarily consists of fan noise at approach and fan exhaust and jet noise at the sideline [12]. The maximum jet sources are generally to be found 5 to 7 nozzle diameters downstream [12].

3.1 Airframe

Previous studies by DLR, NASA, MIT and Boeing among others regarding noise reduction were assessed and evaluated, laying the foundation for the U-Liner's airframe design. It is generally considered that Blended Wing Bodies (BWB) offer the most promising airframe noise reduction capabilities due to the large planform noise shielding and effective low-speed lift generation [1]. These noise levels are currently only matched by the MIT Double Bubble concept which is predicted to emit 213 EPNdB cumulative [13]. These noise level predictions however are considered to be rather optimistic [1], nonetheless the Double Bubble concept serves as a baseline for noise level predictions due to its similarities in airframe design and turbofan placement.

Although BWB noise emissions are predicted to be far superior to current tube-and-wing configurations they fail to meet the market requirement of being family concept-friendly. Even if scaling the BWB was an option, development and production times and costs become unusually high. In contrast to conventional tube-and-wing configurations, the individuality and size of BWB airframe parts presents a major issue even for advanced production techniques such as 3D printing. Furthermore its unfavorable cabin pressure loads imply a massive weight penalty which ultimately recommends a hybrid wing body design with a tube-like fuselage instead of a flying wing. This design approach also resolves the BWB issue of problematic emergency egress solutions.

The aerodynamically required higher incidence angle at takeoff or landing lowers the comfort level of passengers and the crew. Evacuation time with an extraordinary wide inner body, increases drastically [14]. Therefore a 7.3m wide lifting body is designed primarily with regard to its engine noise shielding capabilities. In addition, it offers a viable option for the high-density configuration with 300 passengers in a single-class configuration, bearing in mind airport box compatibility.

The smooth fairing between the fuselage and the wing is derived from BWB designs to minimize airframe noise and interference drag. As the thick wing root requires hybrid laminar flow control to minimize its drag, it also enables new approaches to hybrid propulsion arrangements.

Combining the rear mounted engine with the U-Liner's high wing position ultimately allows the application of a light, small size landing gear. The highly turbulent flow around the undercarriage causes it to be a primary source of airframe noise during approach. The U-Liners main landing gear therefore is equipped with a 'toboggan' fairing which is found to be at TRL 7 [15, 16]. Since the Double Bubble already accounts a 1.9dB noise reduction for the application of faired undercarriage compared to its baseline aircraft [13] no further improvements are assumed for the U-Liner.

3.2 Propulsion System

The U-Liner introduces a turbo electric distributed propulsion (TeDP) system that incorporates an advanced turbo fan (TF) technology and six distributed electric fans (EFs). The EFs are located in the thick inner part of the wing and in the rear section of the aircraft. The single TF is located on top of the upper rear section allowing the ultra wide body to shield agains jet, fan and turbine noise. Additional noise shielding is provided by the vertical stabilizers as well as by positioning the TF two diameters upstream of the tail's trailing edge. This measure is estimated to reduce fan exit and core noise by up to 9.6dB [1].

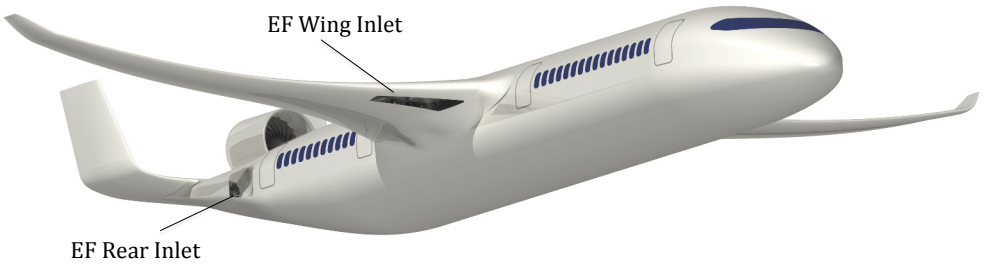

Figure 2: Electric Fans Inlet Positioning

The combination of six distributed EFs and a single TF engine with a design bypass ratio of 16.6, offers great potential to minimize noise levels by increasing the overall engine air flow and therefore reducing the engines specific thrust and outlet velocities. As illustrated by equation 1, these factors are most critical for the generation of jet noise [17].

$$OASPL_{jet} \propto 10 * log\left(\left(\frac{FN}{W}\right)^7\right) \tag{1}$$

The GasTurb optimization, which is discussed in more detail in section 6.4, estimates a reduction of engine outlet velocities by up to 60% compared conventional configurations. This significantly improves noise emissions as well as the engine's propulsive efficiency [18, 19].

To fully benefit from the TeDP technology two general drawbacks of hybrid propulsion have to be compensated. First the additional system weight and secondly the conversion loss when transferring energy from the TF to the EFs [20]. The U-Liner concept therefore introduces an EF system that is designed to entirely avoid conversion losses by operating completely separated from the TF system. The EFs support the TF in thrust intense phases during take off and all the way until the top of climb has been reached. The TF then exclusively powers the aircraft during cruise. The additional weight of the electric system however remains within the aircraft and has to be compensated either by improving the engine's efficiency or the aircraft's aerodynamics. Both improvement opportunities are utilized and discussed.

A key design consideration of the U-Liner is the usage of the electric systems during cruise, not for propulsion but for reducing the aircraft's friction drag through the application of hybrid laminar flow control (HLFC) which is discussed in detail in section 4. This combinational use of the electric system represents a new opportunity to compensate its additional weight. It requires an engineering solution that allows the use of the EFs either for propulsion or HLFC. The U-Liner therefore integrates the six EFs into the inner wing and rear section and introduces a variable inlet geometry illustrated for the wing in Fig 3. The two states of the propulsion system differ in the air flow by controlling the in- and outlet flaps indicated in red. During thrust intense mission phases these flaps are open allowing the EF to work as a propulsion system. In cruise when the TF is at its design thrust, it does not depend on the EF support. The variable inlet geometry then closes and only a small amount of the EF's power is used to ingest the boundary layer on the upper front section of the wing to enable HLFC. The additional advantages for the high lift system are discussed in section 4.

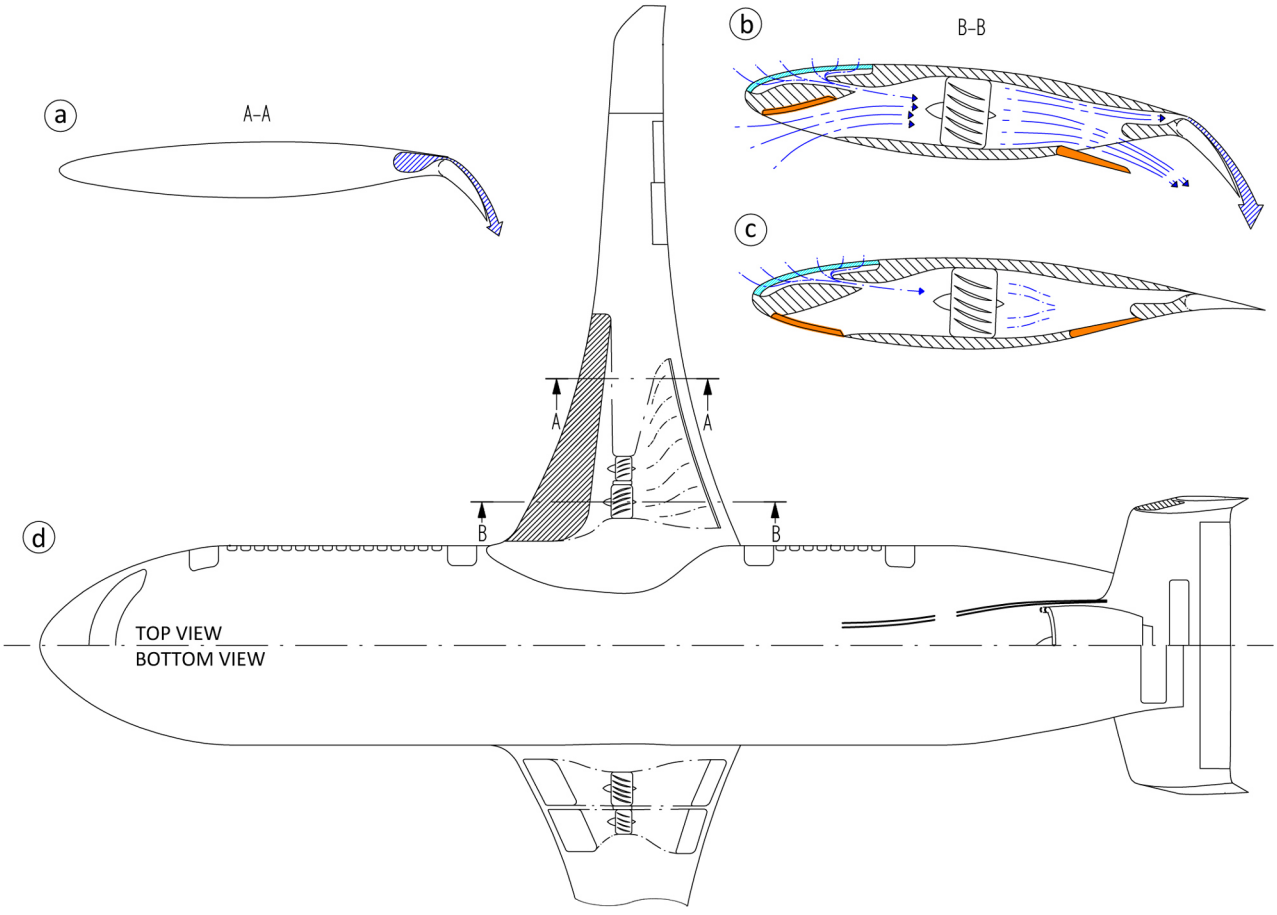

Figure 3: EF Variable Inlet Geometry in the Wing Section

The variable inlet geometry is located on the bottom part of the wing to enable optimal inlet stream conditions for the EF during the propulsion support in the climb sections where the aircraft experiences an high angle of attack. The rear inlets also close during cruise. Their implication on the tail design is discussed in section 4. The propulsion system and all implications of electrical energy as well as a sizing and performance analysis are separately discussed in section 6.

3.3 High Lift Devices

Slotted leading edge devices and trailing edge flaps are major contributors to airframe noise. These become redundant owing to the U-Liner's advanced airfoils as well as adaptive trailing edge structures in combination with the electric fan integration. Natural laminar flow (NLF) airfoils generate sufficient lift to eliminate the need for a leading edge high-lift device [1]. Additionally, they result in considerably lower friction drag.

To provide enough lift at low speeds, the wing's trailing edge is continuously flexed instead of using conventional slotted flap mechanisms. These morphing trailing edge devices offer the possibility to eliminate noise caused by slots and flap track fairings. Previous research [21, 22] and testing in operational environments [23] demonstrated the feasibility thereof. The high lift coefficient required for low-speed lift generation is not only achieved by the morphing flap but also through blowing air onto the flexible trailing edge surface. This circulation control system as seen in Fig 3(b) increases the impulse of the boundary layer, delaying the flow separation. Thereby the flap effectiveness and in turn the overall lift coefficient are increased. Eventually the high lift coefficient allows for landing speeds as low as 120kts, reducing approach noise by 4 EPNdB compared to a common 140kts approach [12].

Furthermore, passive trailing brushes have the potential to almost completely eliminate source noise [9]. Model aircraft experiments thereof reveal a possible reduction of up to 4dB [24], operational implementation of these polypropylene or metallic fibers however remain yet to be investigated.

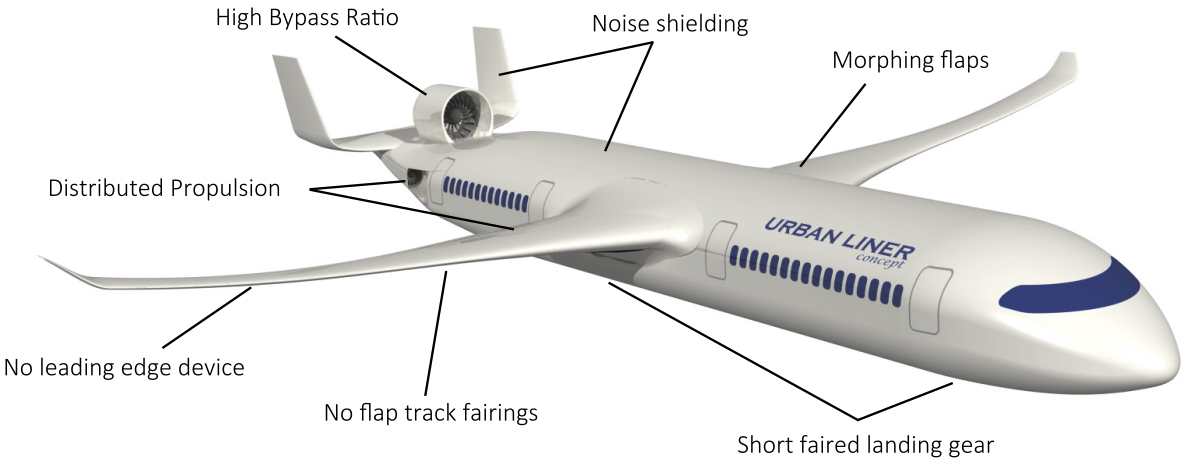

Figure 4: Noise Reduction Technologies

3.4 Operational Noise Savings

Perceived noise levels can be lowered within airport regions not only by airframe and propulsion design but also through optimized approach procedures. Staying at cruise altitude longer and performing a steep low-drag low-power approach can reduce noise levels up to 3.9dB while having minimal impact on flight time and fuel consumption [25]. This matches the estimated 3dB noise reduction of the Double Bubble which are taken into account on the basis of a steep 4 degree approach trajectory [13]. These flightpaths in combination with optimal deployments of high-lift devices and landing gear as well

as accurate approach speeds allow for minimization of noise impact through low noise augmentation systems [25].

Effective perceived noise levels are time-integrated sound levels. The approximated dependence on the distance between the moving aircraft and the observer is between the first and second power [26]. Hence by increasing the climb rate, community noise can be lowered. The high total thrust generated by the TeDP enables take off field lengths of 1500m and climb rates of 2800 ft/min, increasing the distance to the noise measurement point located at 6500m from the runway start compared to current aircraft.

The combination of multiple noise-reducing components results in an overall effective perceived noise level well below ICAO Stage 4 limits, however more precise estimations require CFD simulations and wind tunnel tests which have not yet been conducted at this time. Additional effects caused by the electric fan integration such as mechanically induced vibrations and noise due to electromagnetic field generation remain to be assessed.

4 Aerodynamic Layout

For the U-Liner's aerodynamic layout two primary design targets are the reduced fuel consumption and the low noise footprint. In order to achieve these goals it is essential to reduce the overall drag of the aircraft and eliminate primary noise sources of the airframe. This is achieved by exchanging the conventional flap track systems with a continuously deformed wing skin structure referred to as morphing wings. Effects of this feature are discussed in section 4.4.

The two most significant contributors to the overall drag are viscous drag with more than 50% and induced drag with approximately 30% [10]. To achieve an improved aerodynamic performance these have to be reduced. The share of friction drag plays a dominant role during cruise which accounts for most of the mission time. Lowering friction drag therefore has great potential to reduce fuel burn, emissions and costs.

The motivation behind laminarization is the reduction of friction drag achieved by a laminar boundary layer. Surfaces with a laminar boundary layer have nearly an order of magnitude less friction drag than surfaces with a turbulent boundary layer [27]. Laminarization generally has an increasing effect for larger size aircraft. Based on research regarding laminar flow on transport aircraft surfaces [10,28–35], an aircraft in the U-Liner's size and weight category is expected to achieve a 15% L/D improvement through laminarization. This would result in a 15% reduction in fuel consumption. As mentioned in section 2 laminarization is a key feature of the U-Liner's aerodynamics. The effects and associated theories of laminarization therefore are discussed in the following section.

4.1 Natural and Hybrid Laminar Flow Control

Natural laminar flow (NLF) is a passive technique that uses optimized pressure gradients to maintain a laminar boundary layer. For active boundary-layer flow control (LFC), suction is applied through small holes in the wing's upper surface area to maintain the laminar state at high Re numbers. Three main types of instabilities that cause boundary layer transitions have to be kept in mind [10]. The Tollmien-Schlichting instability (TSI) and Cross-flow instability (CFI) are closely related to the LE sweep angle. Attachment Line instability (ALI) is caused by the fuselage boundary layer disturbances along the wing's leading edge. The Re number and related sweep angle of their occurrence is represented on Fig 5 [10].

Relatively low chord lengths with the corresponding low Re numbers or small leading edge sweep angles allow the laminar boundary layer to be passively maintainable up to a desirable distance from the leading edge. With increasing Re numbers laminarization is only achievable with active flow control. In order to reduce the flow control system complexity hybrid laminar flow control appears to be the most promising technique.

For hybrid laminar flow control (HLFC), increased suction is applied in the leading edge region to prevent transition caused by CFI and ALI. After the active boundary layer ingestion section, wing shaping for favorable airfoil pressure gradients allow NLF over the wing box region, which removes the need for an in-spar suction system.

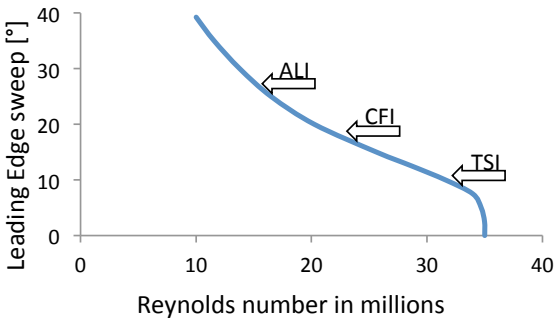

Figure 5: Laminar Flow Boundaries

As the U-Liner's wing houses the EFs, an increased root chord length is required. With the U-Liner's taper ratio this in turn allows the above mentioned HLFC until 50% of the half span, as seen on Fig 3. On the outer wing area, starting at a chord length where NLF can no longer be maintained, the boundary layer is passively controlled.

4.2 Airfoils for NLF and HLFC

Maintaining laminar flow is strongly dependent on the pressure gradient, which is in turn dependent on the flight Ma number. The German Aerospace Research and Test Institution developed a high *Re* number NLF airfoil, with a cruise Ma 0.74 and *Re* number of 26.5e6 [31]. These values are very close to the U-Linerś NLF wing section. This DFVLR-LV2 NLF airfoil was therefore selected for the design.

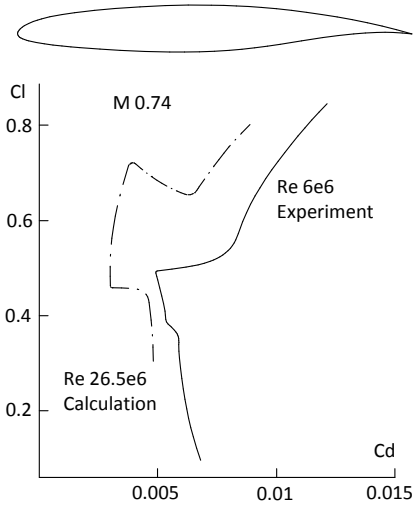

Figure 6: The NLF Airfoil and its Polar

The airfoil's lift curve slope illustrates the potential benefits of NLF with the reduced drag section, the so called laminar bucket. The wing loading was determined to keep the U-liner's outer wing section within the beneficial lift curve area. This is in accordance with the desired elliptical lift distribution of its wing that results in the lowest possible induced drag during cruise. The outer airfoil sections have a negative twist with respect to the root airfoil, and in turn operate with a reduced lift coefficient. The decision for the above mentioned airfoil was verified [36] regarding a future green regional aircraft design. In the research the same airfoil was applied for service conditions of Ma 0.74, *Re* 21e6. For the U-Liner outer wing's NLF section these values are Ma 0.747 with *Re* numbers ranging from 20e6 to 10e6 according to the airfoil section's chord length.

Desirable pressure distribution of HLFC airfoils have been described by NASA [37]. A high capacity HLFC transport aircraft study [27] was the primary source for the U-Liner's HLFC airfoil. The airfoil is designed for cruise conditions of Ma_{3D} 0.8 with Λ_{LE} of 28°. The corresponding 2D values are similar to the U-Liner's HLFC wing section with a general leading edge sweep of 18° and Ma_{3D} 0.75. Again for the preliminary design, this airfoil was selected with thickness adjustments due to structural reasons. The modified HLFC airfoil is illustrated in Fig 3.

After the selection of the NLF and HLFC profiles, with their resulting thickness value it is possible to determine the sweep angle required to keep the wave drag as low as possible. At the modified HLFC profile section a higher sweep angle is required due to its higher profile thickness relative to the NLF

section of the U-Liner. As wave drag of a subsonic aircraft accounts only for a small percentage in the overall drag value it is only mentioned that laminar profiles, such as transonic designs, expand the drag divergence Ma number further [10]. Reduction of the cruise Ma number from the conventional 0.8-0.85 to 0.75 allows using smaller leading edge sweep angles, which benefits the laminar flow around a NLF wing. This reduced sweep angle in turn reduces wing weight, increases maximum lift coefficient and reduces terminal noise footprint. The sweep angles have been defined with the help of Torenbeek's equation [38] for supercritical 2D sections and later on verified with Korn's equation which is based on empirical data of second generation supercritical airfoils [39].

4.3 Wing Design

The U-Liner's wing system as schematically represented in Fig 3 uses the EFs located in the wing to produce the required ingestion force for the HLFC control during cruise. The ingested airflow is used to eliminate the bleed air requirements of the turbofan engine during cruise. At takeoff and landing where the mass flow for the EFs is greatly increased, additional inlet and outlet slots are opened at the lower surface of the increased incidence wing. This was discussed in section 3.2. The HLFC mass flow from the front upper surface is than additionally led to the inlet opening mass flow, constituting together the overall mass flow required for the EFs. The accelerated outlet airflow is deflected into two parts. It produces the required blowing mass flow for the circulation control wing (CCW) system, and produces thrust while exiting the aft section of the wing. The lower maximum angle of attack due to the NLF profile could be compensated by the U-Liner's wing configuration, as the CCW technology increases high lift coefficients, even at moderate angle of attacks. This enables the U-Liner's NLF wing section to generate more lift during takeoff and landing and enables the operational request for short runway lengths.

4.4 High Lift System

A promising solution for reducing mechanical complexity of conventional high lift systems is the CCW concept. This employs tangential blowing over the trailing edges through slots and prevents trailing edge separation, thus encouraging favorable pressure gradients for high lift coefficients. Combined with leading edge blowing 2D lift coefficients greater than 7 are realizable. With moderate blowing rates lift coefficients greater than 3 were measured at 0 angle of attack [40,41]. Tests to measure the lifting capability of a 3D CCW wing resulted in lift coefficients exceeding 5 [41]. Pneumatic leading edge devices were identified to have a remarkably greater effectiveness than the Kruger flaps used in the reference configurations [40].

The application of CCW in the U-Liner greatly lowers takeoff and landing speeds which in turn reduces the required runway lengths and enable a smaller noise footprint due to steep climb out and eliminated flap tracks [41]. A NASA study evaluated the effectiveness of applying this concept to a Boeing B737 wing. The typical 15 moving elements per wing were replaced with the CCW flaps and leading edge system, resulting in a maximum of 3 moving components per wing [42]. This emphasizes how strongly the high lift system complexity is reduced with the use of CCW technology. The U-Liner's pneumatic leading edge device is the frontal upper suction area. This is not only beneficial as no other leading edge high lift system has to be installed, but also because the energy requirement for relaminarization accomplished with leading edge blowing could typically be an order of magnitude greater than the energy requirement of delaying separation achieved with suction [43] . Fig 3 represents the above mentioned high lift systems incorporated in the U-Liner's wing.

4.5 Wing Drag Reduction

The induced drag of a long-range transport aircraft at cruise conditions is the second largest contributor to total drag. This value is much greater at low speeds where it may account for 80% to 90% of the aircraft's total drag [10]. A typical way to decrease the lift-induced drag is to increase the aspect ratio of the wing. However wing aspect ratio is a compromise between aerodynamics, structure characteristics and operational aspects such as the airport gate sizes. The alternative is

to develop wing-tip devices acting on the tip vortex. A parametric study was done to research the relative advantages of winglets and wing-tip extensions [44]. The results illustrated that for most tip extension a better performing winglet is found. For the preliminary design of the U-Liner a blended winglet is incorporated with a height of 6% of the half-wing span. This wing tip geometry is estimated to result in an induced drag reduction by 4% [34].

One of the reasons for the high wing location is its aerodynamic efficiency as 60% of the lifting force is generated on the upper surface of the wing. A high wing configuration maximizes the usable upper wing surface. For this reason the U-Liner has a higher maximal lift coefficient and in turn lower approach and stall speeds than conventional configurations. ONERA conducted a study on the wing body fairings for high wing subsonic aircrafts. The resulting optimal shape which is comparable to the U-Liner reduces interference drag by 8% [45].

4.6 Lifting Fuselage Design

Aerodynamic shape optimization for transport aircraft results in a more slender lifting center-body with distinct wings [14]. As a consequence and because of the difficulties related to BWBs, the optimal solution to meet the operational and low noise requirements is a configuration with increased fuselage lift but a separated wing section. The U-liner's final fuselage design benefits from the following aerodynamic effects:

- The higher carryover lift enables the reduction of the exposed wing area and its weight and reduces the induced drag [46]
- Following the design aspects of a tailless airplane the fuselage's centerline is reflexed for pitch trim, which shrinks the required horizontal tail size and download
- The shorter cabin reduces the CG range, further shrinking the tail [46]
- Engine positioning reduces the engine-out yaw moments, shrinking the vertical tail area and weight

It has to be highlighted that the wetted area determines friction drag, while induced drag is inversely proportional to span. As a consequence a higher wetted aspect ratio (AR) is desirable. A comparison of wetted AR vs. AR of reference configurations is represented in Fig 7. This figure underlines that a configuration between classical tube-and-wing and BWB is a desirable solution.

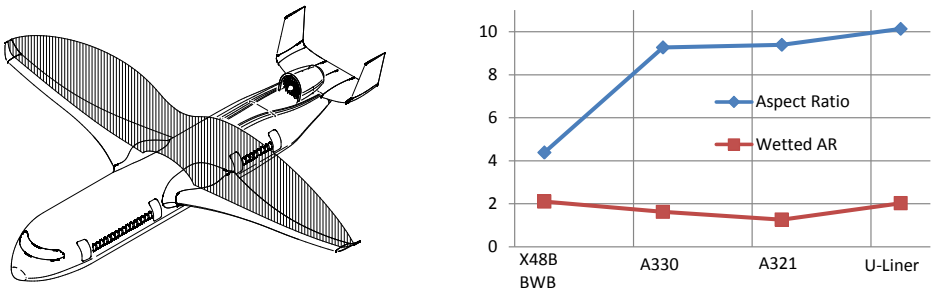

Figure 7: Lift Distribution and Aspect Ration Comparison

The upswept aft fuselage surface typically contributes to the form drag of the aircraft, and causes the generation of vortices to form on the underside of the aft fuselage. One of the most promising solution for this problem is the usage of small strakes published recently as the Microvanes [47]. Bonding these strakes onto the aft fuselage on either side of the bottom section slows the vortex formed by the upswept aft of the aircraft. For a high wing aircraft this solution is estimated to allow a 3% reduction of cruise fuel consumption [48].

4.7 Reduced Tail Size

Laminarization of the tail surfaces and nacelle provides a significant reduction of the overall drag of the airplane [10,28–35]. Reducing the wetted area of the tail lowers the overall drag even further. Its profile drag and the increase of induced drag from the tail download both directly lower the overall C_L/C_D. The wetted area reduction therefore is one of the driving factors for the development of the flat rear fuselage airplane with the integrated empennage concept of Airbus [49]. Similarly to the HLFC fin of the A320 [50], the U-Liner's vertical tail surface has a leading edge sweep that is too high for the adherent Re number to enable natural laminar flow. This requires active laminar flow control to maintain a laminar boundary layer on the U-Liners vertical tail. The high lift coefficient of the wing during landing has to be balanced by the tail. To realize a reduced tail size, blown elevator control surfaces are required. The system is represented in Fig 8. At the outer section (A-A), only a blowing plenum is used to reduce the system complexity. As the U-Liner uses its EFs for landing the generated airflow is partly deflected to the upper surface of the horizontal tail. The purpose of this is to outweigh the shielding effect of the windmill-state TF engine and to increase the dynamic pressure on the surface.

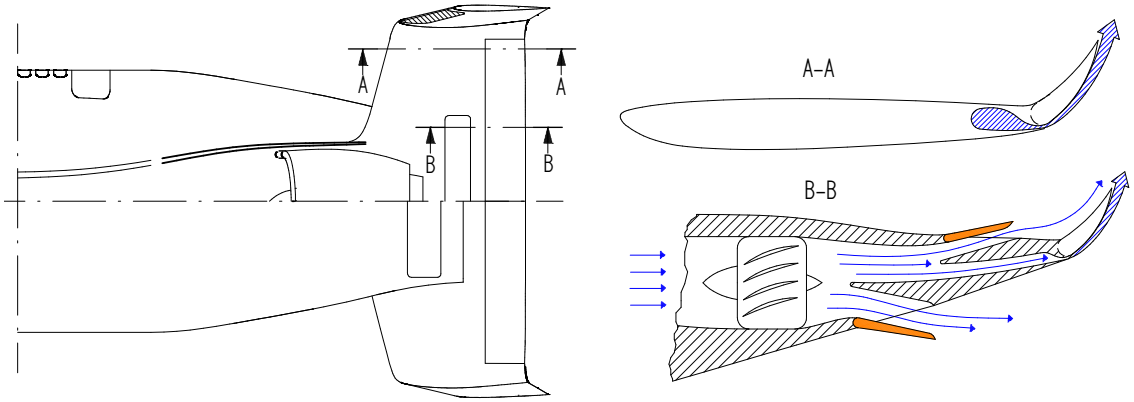

Figure 8: Horizontal Tail Lift System

As a secondary effect thrust vectoring of the EFs occurs as a result of the elevator deflection. For blown trailing edge surfaces with no leading edge device an increase of ΔC_L of 2 is achievable [51]. As a consequence for the U-Liner's tail $C_{Lmaxtail}$ 3.7 was assumed for further analyses.

If active stability augmentation systems are involved in the initial aircraft design the static margin (SM) can be reduced to lower values [52, 53]. This allows a reduced tail size which also reduces the tail weight. Due to lower SM reduced tail download is required and the induced drag decreases. For a transport aircraft the tail is typically sized by the maximum required download at landing.

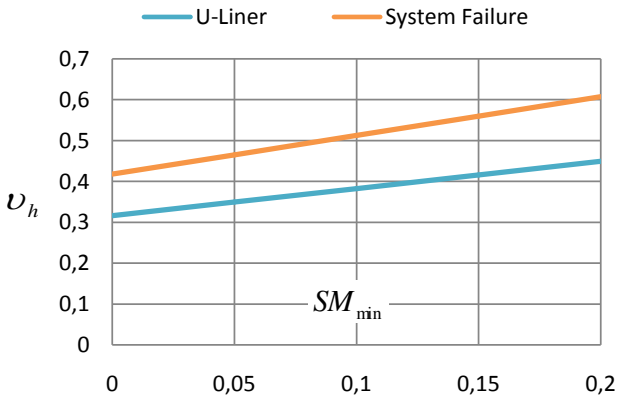

Figure 9: Horizontal Tail Volume Coefficient

Following the usual pitch-trim and pitch-stability relations [46], the horizontal tail volume coefficient of the U-Liner with respect to static margin is presented in Fig 9. It is illustrated that under normal operating conditions due to the greatly increased lift coefficient of the tail, a relatively low tail volume coefficient ν_h is sufficient. The U-liner's tail was sized with its ν_h of 0.518 to maintain a safe landing in case of an electric system failure interrupting the airflow for the blown tail high lift system. A safe landing can be executed even if the slot blowing system of the elevator entirely fails. In this emergency situation the high lift system of

the wing is not applied, in order to reduce its maximal lift coefficient that has to be counterweighted by the tail surface. This situation requires a high speed emergency landing but does not impose a safety critical event.

	C_{Lmax}	$C_{Lmaxtail}$	SM	$\Delta x_{cg}/c$	Required ν_h	Actual ν_h
Active Systems	2.8	3.7	0.1	0.51	0.41	0.518
Failure of Systems	1.6	1.4	0.1	0.51	0.51	0.518

Table 1: Required and Actual Horizontal Tail Volume Coefficient

To reduce the complexity of the horizontal tail the use of active flow control next to the blown plenum system was avoided. In case the elevator blowing plenum system fails, the airfoil has to provide adequate low speed properties to counterbalance the lift generated by the wing. The objective of the tail design was to select an airfoil which is a satisfactory compromise between high speed and high lift values, as these values are generally in conflict to each other. Following a study for reducing tail size of commercial aircraft [53], a helicopter rotor blade was selected as an initial design for the tail's airfoil. This airfoil is represented in Fig 8. For the U-Liner's reduced tail size the wide range of aerodynamic conditions appearing in a single cycle of a helicopter rotor blade (forward running higher speed blade with opposite side rearward running lower speed blade) represents a suitable airfoil design.

Table 2 contains the static longitudinal and directional derivatives of the U-Liner and a comparison to their typical values according to Sadraey [52]:

Requirement	Symbol	Typical Value $(1/rad)$	U-Liner
Static Longitudinal Stability	$C_{m\alpha}$	-0.3 to -1.5	-0.53
Static Directional Stability	$C_{n\beta}$	0.05 to 0.4	0.12

Table 2: Stability Derivatives of the U-Liner

4.8 Estimation of Maximum Subsonic L/D

For a rough estimation of the maximum aerodynamic efficiency a two term approximation of the drag polar as mentioned by Torenbeek [10] is applied.

$$\left(\frac{c_L}{c_D}\right)_{max} = \frac{b_w}{2}\sqrt[2]{\frac{\pi\, e}{c_{feq}\, S_{wet}}} \tag{2}$$

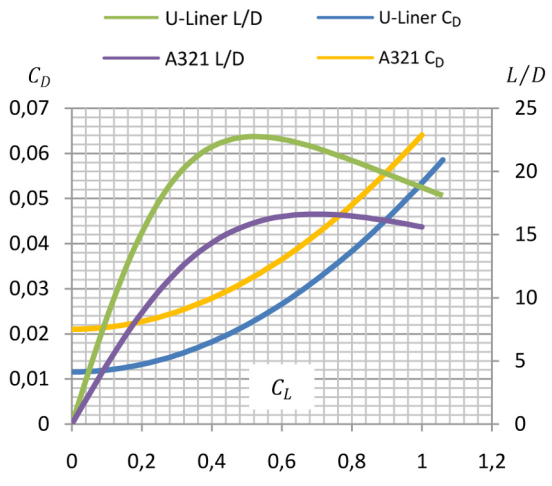

Figure 10: Lift over Drag Comparison

C_{feq} represents the equivalent skin friction drag coefficient based on the total airplane's wetted area. Extracting the friction drag coefficient from research data based source [54] and assuming fully turbulent surfaces, C_{feq} is equal to 0.00316.

A detailed zero-lift drag calculation was conducted based on the Component Buildup Method from Raymer [55] which allows to include the effect of laminarization in the calculation with turbulent and laminar flat-plate skin friction coefficients for each main component of the aircraft.

The drag polar in Fig 10 is determined based on the form factors, component interference factors and the additional drag due to the upswept aft fuselage section. For a comparison the Airbus A321's polar is calculated using the equivalent skin friction coefficient and span efficiency factor according to Raymer [55]. The above mentioned drag reduction technologies of HLFC and the reduced tail size drastically improves the L/D of the U-Liner compared to the A321. Hence a L/D of 23 appears to be a realistic assumption for the U-Liner concept.

5 Structural Optimization

The structural layout is based on the aerodynamic design, bearing in mind operational conditions and production feasibility. In order to achieve the specified emission goals and payload capabilities, aiming for low structural weight is crucial. Therefore the U-Liner relies on the efficient application of fibre-reinforced polymers. The fuselage and wing structures are made from fatigue-resistant carbon fibre composites which simultaneously allow for higher humidity within the cabin compartment and therefore greater comfort. Monolithic composites are applied in areas that are exposed to high shear stresses like the wing root whereas sandwich constructions lower structural weight where bending is the primary load form, including the wing's leading edge as well as the folding wing tip. Applying sandwich constructions in load bearing components is currently prohibited by regulatory constraints however are deemed necessary in order to reach the aspired objectives set by international organisations. On top, technological improvements in simulating and making use of the material's anisotropy is factored with a 10% improvement regarding mass estimations.

5.1 Load Alleviation Systems

The wing root bending moment represents a design driver regarding the structural layout of the wing. For the purpose of weight reduction, load alleviation systems find application on the U-Liner. These offer the possibility to lower bending moments without adding mechanical complexity to the aircraft. Shifting the lift vector closer to the wing root by deflecting ailerons upwards and trailing edge flaps downwards can drastically reduce wing root bending moments [56,57] and thereby make thinner wing skins possible. Previous research shows that load alleviation systems allow for more payload while keeping the vertical load factor constant [56].

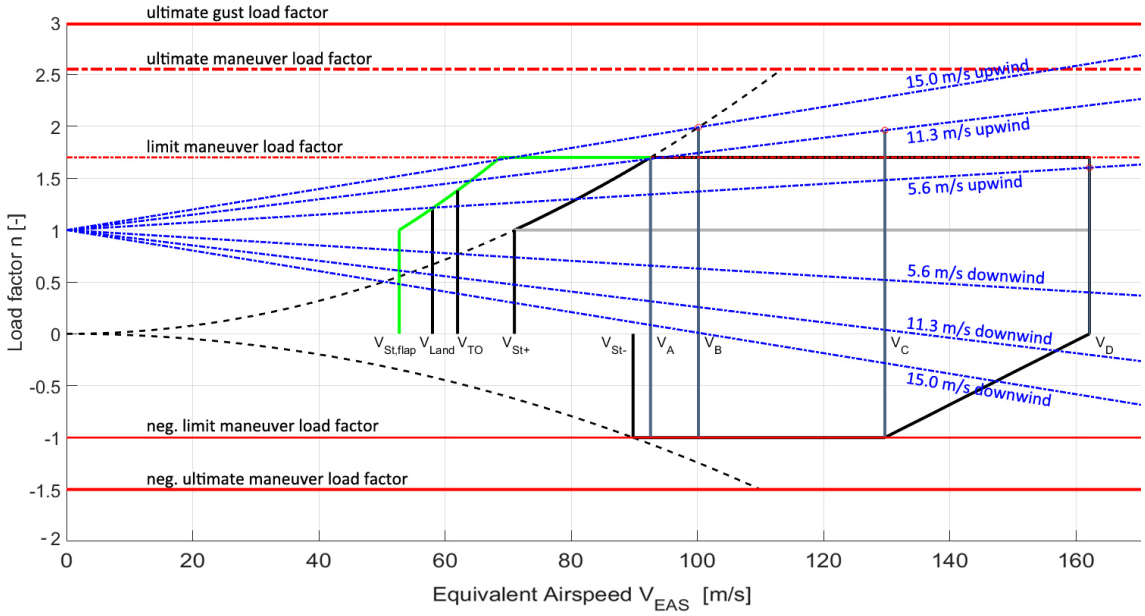

Figure 11: Reduced Vn-Diagram based on Load Alleviation Systems

Compliant with EASA CS25, the aircraft needs to withstand limit loads occurring at 2.5g with a safety factor of 1.5. Active maneuver and gust load alleviation on the other hand guarantee safe operations of the aircraft within a reduced Vn-diagram. The vertical limit maneuvering load factor is therefore lowered from 2.5 to 1.7 while the ultimate maneuvering load factor is adjusted to 2.55, keeping a safety factor of 1.5.

In order for the gust envelope to take into account the load reductions from the gust load alleviation system, a linear dependency of gust loads on gust speeds is assumed [58]. Reversely the relevant gust speeds are lowered linearly with the load reduction potential of the system for a Vn-diagram integration. Assuming the gust load alleviation system to be able to safely reduce wing root bending moments by 25%, the maximum load experienced by the aircraft at design speed for maximum gust intensity V_B exceeds the maneuver limit load of 1.7. The ultimate gust load factor of 3.0 is therefore more relevant for the structural design as opposed to the ultimate maneuver load factor of 2.55. Applying a system capable of effectively alleviating gust loads, maneuver loads as well as suppress flutter eventually changes the limiting structural specifications to other loads like landing [59].

5.2 Wing Root Design

The smooth interface between the lifting tube-like fuselage and the wing enable the hybrid propulsion arrangement in the first place. On the other hand, the wing is placed at an aerodynamically favorable position three quarters up the fuselage. Consequently, a new approach to the wing root design has been applied. The split root arrangement is easily distinguishable from classical layouts as it is designed to encapsulate the cabin compartment between the upper and lower wing skin. It carries the loads of the upper skin and stringers through the cabin ceiling while the lower wing skin and stringers are guided alongside the cabin floor as seen in Fig 12. The integration height of the electric fans coincides with the cabin middle. Consequently the maximum deflection angles of the upper and lower wing skin are similar. The air intake for the electric fans is mounted through openings in the spars. As the spar webs are insignificant for load handling this only implicates restrictions for the fuel system. The duct inlets at the wing surface are unproblematic from a structural point of view because both leading and trailing edge surfaces are not carrying any significant loads.

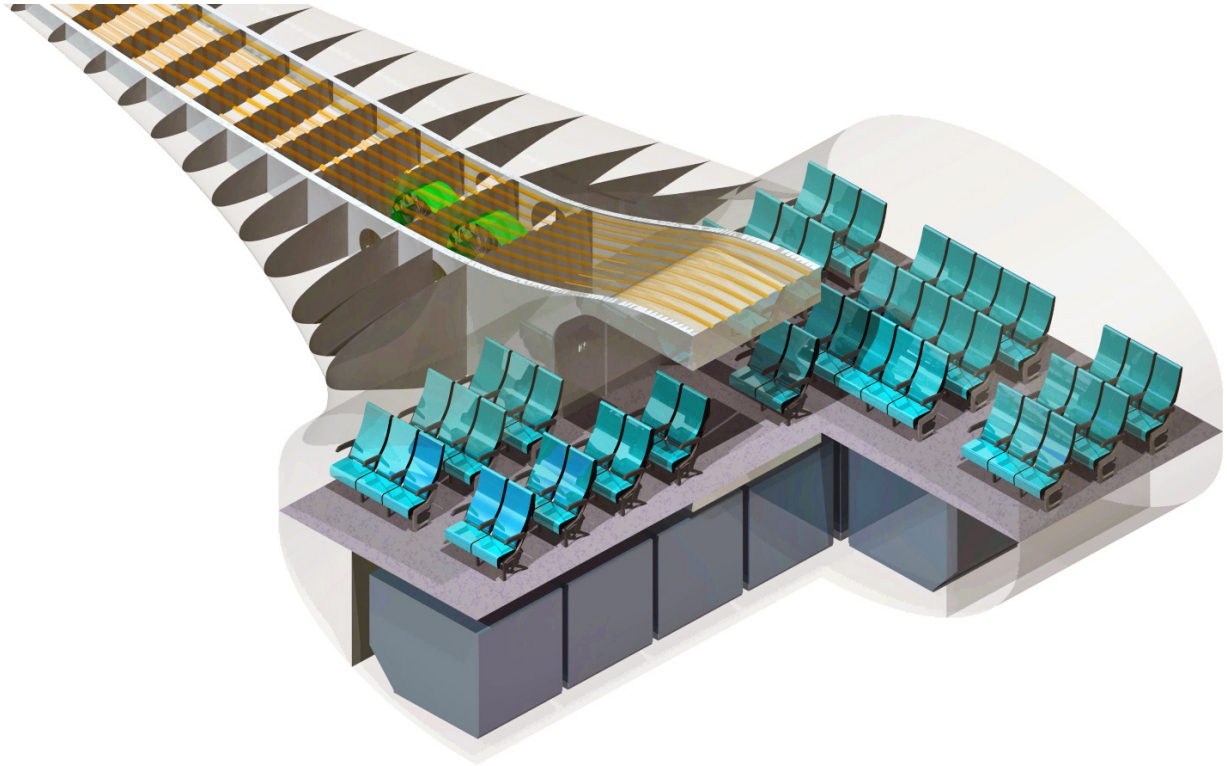

Figure 12: Wing-Fuselage Intersection with EF Integration

The low sweep angle minimizes structural weight by requiring only 8 omega stringers which offer optimal torsional stiffness. Taking into account also the missing landing-gear integration at the wing, no additional spar at the wing root is necessary. The front and rear spars are supported further into the cabin compartment through additional walls without interrupting the available cabin or cargo space, eventually reaching the central axis where they are joined with their counterpart to create a continuous load transfer. In order to evaluate the concept, analysis regarding buckling, material stresses and deflections were conducted by the means of Finite Elements Methods (FEM). To make use of the same model for both FEM and future Computational Fluid Dynamics simulations, the wing is modelled in between jig- and flight-shape.

Since the wing root's moment of inertia is extraordinarily high as a result of the encapsulated cabin, the design driving load case for wing skin thickness is buckling. The structural layout has been engineered to prevent local as well as global buckling by shifting the critical eigenvalues beyond 1 for a limit gust load. At the leading and trailing edge this is primarily achieved through sandwich constructions. The spars and wing skin are monolithic laminates mainly due to the difficult load transfer into sandwich panels. Composite stresses caused at 2g are found to be insignificant for component sizing compared to buckling. A representative wing lift distributions results in material stresses well below first failure stresses.

At the attachment of the top wing skin to the fuselage, span-wise wing stringers and longitudinal fuselage stringers intersect to prevent the area from buckling however only the influence of the wing stringers was investigated.

Another key feature of the U-Liner concept are the folding wingtips. The outermost 4m each side are folded downwards prior to reaching the parking position in order to fit inside the airport boxes previously discussed. Downward-folding is enabled once again by the high wing position and favors load distribution at the hinge compared to upwards folding. The fuel tanks are placed between the outer electric wing-fan and the hinge for the folding wingtips while the space between the innermost rib and the fuselage is preserved for batteries to constantly counteract the wing root bending moment.

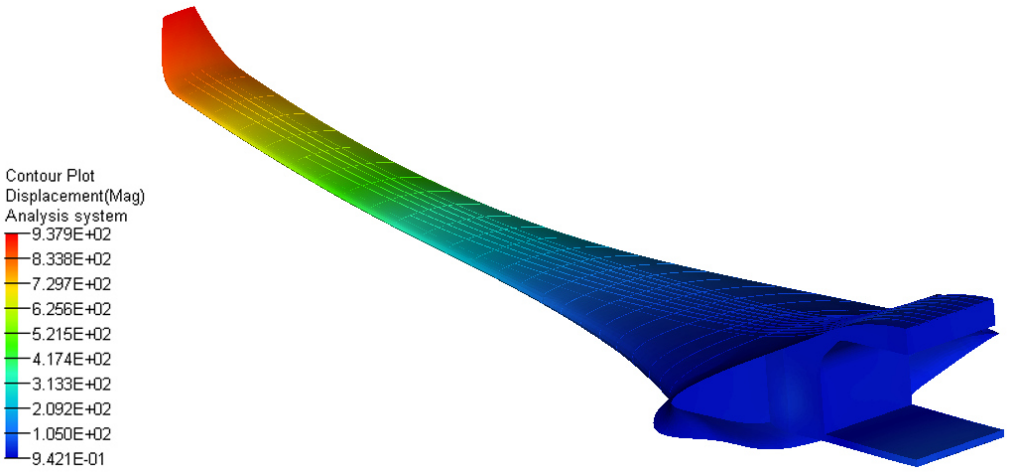

Figure 13: Wing Displacement [mm] at 2g

5.3 Fuselage Structures

The high wing of the U-Liner not only affects the cargo space but also leads to a landing gear integration in the fuselage and allows for optimal longitudinal positioning as the wing position is no constraint. The freight compartment is interrupted at the integration point to provide enough space for the main landing gear and ensuring an adequate track width. Next to the cargo space, vertical stabilizers assist in bearing the cabin pressure loads of the dual-elliptical fuselage cross section.

Resulting from the high-density configuration of 300 PAX, four type A exit doors are placed on each side of the cabin to ensure safe evacuation. These are embedded in a full composite fuselage

design similar to modern aircraft. The recurring structural pattern aims to reduce production costs while encouraging the family concept design.

Figure 14: High-Density Single-Class Cabin Layout

The unconventional layout of 11 seats abreast keeps the fuselage short compared to current twin-aisle aircraft and can be adapted to 10 seats abreast in either twin- or triple-aisle configuration. The latter arises from the requirement to lower boarding times and thereby enhance profitability.

Single Class	3-5-3	301 PAX
Single Class	3-2-2-3	272 PAX
Two Class	3-4-3 E/C 2-2-2 B/C	232 PAX

Table 3: Cabin Configurations

At the rear of the fuselage, the load transfer from the single turbofan is assumed to be feasible. Without further investigation also the implementation of the electric engine pair at the aft section is deemed unproblematic because of the limited thrust level. The air duct inlets leading to the additional fans require the installation of a hydraulic system. These technologies however exist already and are not assumed to be hindering the concept from a structural point of view.

6 Low NOx Propulsion System

A primary design target of the U-Liner concept is to reduce nitrogen oxide (NO_x) emissions in the near airport environment and during cruise in higher altitudes. Therefore the potential of alternative propulsion technology is investigated and the application of a hybrid electric system further evaluated. The turbo electric propulsion system introduced in section 3.2 is discussed in more detail. This includes a performance assessment to incorporate operational requirements as a baseline for the subsequent component sizing. The resulting electric system is combined with a promising TF technology which is down-selected from a number of multivariable TF cycle optimization studies that were conducted in the simulation tool GasTurb12. The resulting engine performance figures are compared to current TF technologies and potential improvements in efficiency and NO_x emissions are presented.

6.1 Investigation of Alternative Propulsion Systems

To achieve an 80% reduction of LTO NO_x emission hybrid electric energy concepts, hydrogen fuels and fuel cells were examined for alternative aircraft propulsion. Systems however that contain large amounts of hydrogen suffer from severe drawbacks. Most critical is the high operational safety risk, the contrail cloud emission and the increased system complexity especially when incorporating cryogenic tank cooling [4,20]. The hydrogen tanks also cause a noticeable weight penalty to the aircraft. The U-Liner therefore focuses on incorporating electric energy as a possible alternative to TF propulsion.

A key metric for the applicability of electric energy in aircraft propulsion is the specific energy density of batteries. Today specific energy densities of $Li-Ion$ batteries are limited to 200-300 Wh/kg which is approximately 2.5% of Kerosine fuel [60,61]. Improving these energy densities receives a great amount of research attention and technological advancements in battery materials are expected to enable higher densities [60]. Estimations until 2035 mostly range from 500 - 1500 Wh/kg [60]. The most promising $Li-O_2$ combination has the potential to reach up to 1750 Wh/kg [20] but the feasibility of a $Li-O_2$ batteries is highly uncertain and not considered to be a realistic technology for an EIS 2035 Aircraft [20,62]. The U-Liner concept therefore incorporates a more realistic sulfur based battery system which is expected to yield an energy density of 500 - 1250 Wh/kg until 2025 [20].

Based on these estimations an energy density of 1150 Wh/kg is chosen for the EIS 2035 U-Liner concept. This density is far off from the 2000 Wh/kg limit which was identified to enable universally electric flight for short range transportation aircraft [63]. A pure electric design therefore is considered to be infeasible but the combination of electric and turbo propulsion remains as a possible alternative to conventional TF technology. The impact of the energy density on the feasibility of the concept is discussed in a sensitivity analysis in section 7.3.

Introducing electrical energy to an aircraft's propulsion system enables advantages linked to the characteristics of electric motors. Their energy conversion throughout the entire efficiency chain is far superior to a heat engine [20,61]. Maximum available power outputs of EFs may be considered as independent from Ma number and operating altitude when assuming appropriate heat management [61]. This is contrast to turbo engines which depending on their BPR loose about 80% of their thrust output at the initial cruise altitude (ICA) [61,64]. Power densities of normal conducting electric motors range from 2 to 10 kW/kg which is already comparable to gas turbine power densities [60]. Optimistic estimations expect high temperature superconducting electric motors to reach power densities of up to 40 kW/kg until 2035 [60]. These systems however rely on advanced cryogenic cooling techniques which introduce a high level of system complexity to the aircraft [65]. This complexity has to be controlled in order to enable the technology for application in transport aircrafts. The U-Liner concept therefore relies on a rather conservative power density estimation of 3.8 kW/kg including motors, cooling, cables, inverters and crosslinks.

6.2 Performance Baseline

With the U-Liner competing in a short to medium range market segment it has to deliver flight performance figures that are similar to an Airbus A320 type aircraft. The mission profile in Fig 15 lists the climb performance figures of the U-Liner and the ROC figures of a short range reference aircraft as a comparison. The reference data is taken from the CeRAS database [66]. The table contains only data that is relevant for sizing the components of the propulsion system. This includes all mission segments from taxiing until the TOC as well as the critical OEI case. These represent relevant inputs for the sizing of the battery system. Descent, loiter and approach however do not effect battery sizing due to the large ETOPS reserve of the OEI case far surpassing the amount of energy required for these flight segments. They also do not effect the sizing of the electric motors due to their part load characteristic.

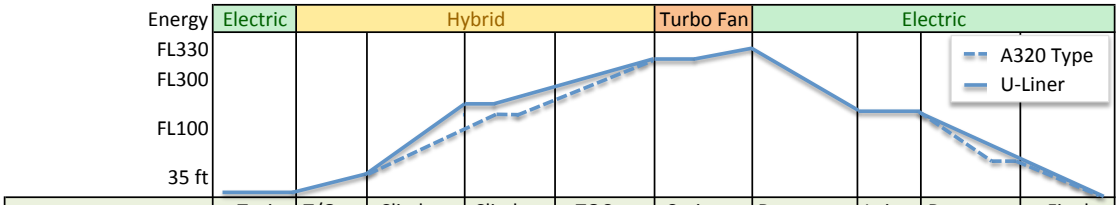

Mission Phase	Taxi	T/O to 35 ft	Climb to FL 100 (3000m)	Climb to FL300 (9000m)	TOC at FL350 (11000m)	Cruise at FL300-FL350	Descent to FL100	Loiter	Decent to 1500ft	Final Approach	ETOPS 90
Time [min]	26	0.7	4	11	7	460	-	-	-	-	90
ROC A320 [ft/min]	-	400	2400	1800	1200	500	-	-	-	-	100
ROC U-Liner [ft/min]	-	400	2800	1600	1200	500	-	-	-	-	100
ROC U-Liner [m/s]	-	2.0	14.0	8.0	6.0	2.5	-	-	-	-	0.50
Airspeed [knots]	25	120	250	310	310	Ma 0.75	-	-	-	-	-
Airspeed [m/s]	13	60	130	160	160	220	-	-	-	-	167.20
SEP Rate [m/s]	-	8.00	15.58	8.67	5.77	-	-	-	-	-	0.76
Sizing Constraint	-	TET	E-Power	-	-	TF Thrust	Irrelevant for Sizing (-)				Battery

Figure 15: Mission Profile

The operational requirements from the mission profile are processed into two separate performance assessment charts in Fig 16. The left chart contains all sizing constraints for take off, the right chart

all constraints during the climb segments.

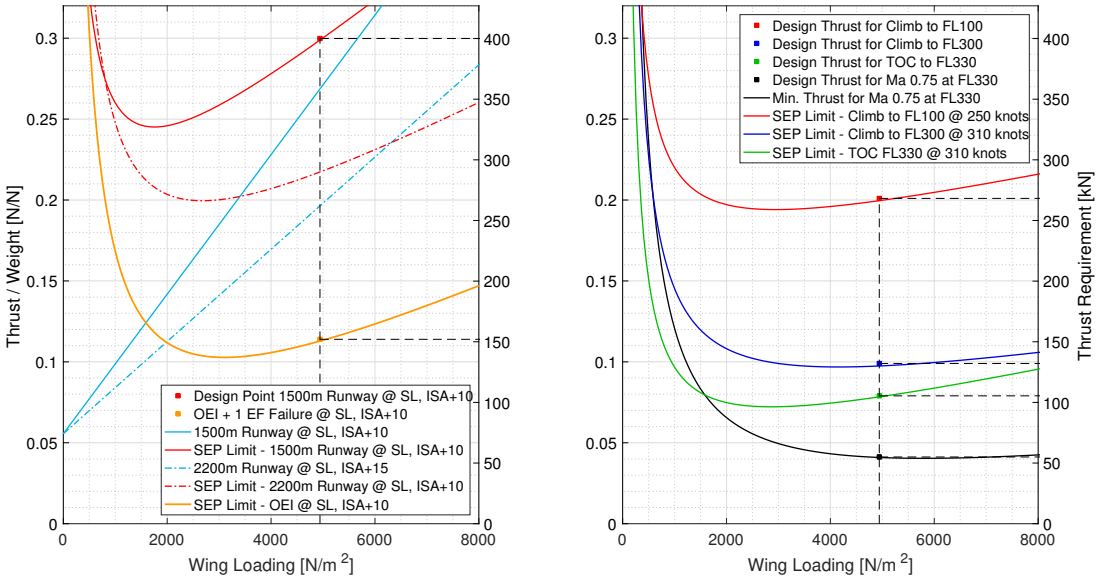

Figure 16: Performance Assessment Charts

Two basic figures of merit used for the performance assessment are the aircrafts wing loading and specific excess power (SEP). SEP represents the utilizable energy difference at a specific point in time it can be used for acceleration or climb power.

$$SEP = \frac{dH}{dt} + \frac{V}{g} \cdot \frac{dV}{dt} \tag{3}$$

The SEP curves in the take off chart on the left side of Fig 16 represent the thrust required for accelerating to take off velocity and reaching the 35 ft altitude. The runway curves represent the distance required for the Aircraft to lift off. They include a safety factor of 1.2 to account for the acceleration-stop distance [58]. The design point for take off illustrated by the red dot, is driven by the required SEP to accelerate to take off velocity on a short 1500m runway. The resulting thrust to weight ratio of the U-Liner is above the limit for a typical 2200m runway limit [66]. Fig 16 illustrates the strong dependency of the SEP and runway limits on the aircraft's wing loading. This was incorporated as a key factor for the U-Liner's wing design.

A critical design point for every propulsion system is to ensure a safe take off even in the unlikely event of an engine failure. In order to comply with FAA and ICAO regulations the remaining SEP for OEI has to ensure at least a ROC of 100 ft/m [67]. For hybrid configurations this SEP minimum most often imposes a critical sizing constrain on the secondary power systems [68]. Fig 16 illustrates the SEP limit for the OEI case as a lower boundary for the secondary power system. To ensure additional safety the U-Liner aims to achieve this minimum even if the TF and one EF fail.

The performance analysis on the right side of Fig 16 determines the thrust levels required to achieve the pursued climb performances. A major design targets is to increase the maximum ROC from take off to FL100 by 20% in order to minimize noise levels in the near airport environment. This climb segment requires the maximum SEP and therefore imposes a critical sizing constrain on the overall propulsion design. The high ROC to FL100 allows the following climb segments to be performed with a lower ROC requiring less SEP to reach the cruise altitude. The design thrust at cruise conditions results from the thrust to drag balance of forces at maximum cruise velocity. It represents the design point for the TF System and is the baseline for all cycle optimization studies.

6.3 Component Sizing

To size all components of the hybrid propulsion system, the performance figures were taken as a baseline. A major design target is to avoid TF part load conditions and to relocate the TF design point from TOC to cruise conditions. This prevents oversizing and improves cruise efficiency. The TF thrust levels at the different mission phases were determined via a GasTurb simulation in which the cruise condition represented the design point and all other segments were treated as off-design points. The electric system then has to compensate the undersized TF performance during the climb segments and at take off. Table 4 summarizes all required thrust, power and energy demands for sizing the system components.

Mission Phase	Taxi	T/O to 35 ft	Climb to FL 100 (3000m)	Climb to FL300 (9000m)	TOC at FL350 (11000m)	Cruise at FL300-FL350	Descent to FL100	Loiter	Decent to 1500ft	Final Approach	ETOPS 90
Throttle TF [%]	0%	100%	100%	100%	100%	100%	0%	0%	0%	0%	0%
EF Power [%]	3%	79%	93%	43%	48%	3%	-	-	-	-	57.74%
Time [min]	26	0.7	4	11	7	460	-	-	-	-	90
Req. Thrust [kN]	28.02	400.25	262.80	124.20	96.31	54.38	-	-	-	-	48.07
TF Thrust [kN]	0.00	217.53	163.14	87.01	54.38	54.38	-	-	-	-	0
EF Thrust [kN]	28.02	182.72	99.66	37.19	41.93	0.00	-	-	-	-	48.07
TF Power [MW]	0.00	13.05	21.21	13.92	8.70	11.96	-	-	-	-	0.00
EF Power [MW]	0.42	12.60	14.89	6.84	7.71	0.40	-	-	-	-	9.24
TF AUX Power [MW]	0.00	0.60	0.75	0.75	0.75	0.95	-	-	-	-	0.00
EF AUX Power [MW]	0.60	0.00	0.00	0.00	0.00	0.00	-	-	-	-	0.95
Req. E-Energy [MWh]	0.44	0.15	0.99	1.25	0.90	3.07	-	-	-	-	13.86
Req. TF Energy [MWh]	0.00	0.16	1.46	2.69	1.10	99.01	-	-	-	-	0.00
Total Energy [MWh]	0.44	0.31	2.46	3.94	2.00	102.07	-	-	-	-	13.86
Sizing Constraint	-	TET	E-Power	-	-	TF Thrust	Irrelevant for Sizing (-)				Battery

*E-Efficiency η= η_el η_pr = 0.87

E_EL Req. [MWh]	20.66
P_EL/P_Total [%]	0.17

Total Battery Weight @ 1150 Wh/kg

ETOPS 90 [t]	17.96
ETOPS 120 [t]	21.98

E - Motors @ 3.8 kW/kg

Power [MW]	16.00
Weight [kg]	4210.53

Table 4: Electric System Sizing

The electric power requirement P_{el} depends on the EFs net thrust FN, the aircraft's flight velocity V and the product of the engine's electric efficiency η_{el} and propulsive efficiency η_{pr} [68]. The electric energy requirement is determined as the product of the EF power requirement and the time of the flight segment.

$$P_{el} = \frac{FN \cdot V}{\eta_{el} \cdot \eta_{pr}} \tag{4}$$

The increased ROC to FL100 and the substantial EF support during take off require a great amount of thrust but only for a short period of time at low flight velocities. The steep climb angle and the EF support during take off therefore represent a sufficient solution for significantly reducing noise levels by incorporating the advantages of electric propulsion. The resulting TeDP design contains six electric motors with a combined output of 16 MW. This design offers a 25% margin over the OEI minimum and a 10% margin in case of OEI and one EF failure.

A TeDP system with a single large TF instead of two small Turbofans is considered for the U-Liner design. This configuration has a lot of potential for reducing emissions and noise levels. The OEI case however imposes a critical sizing constraint on the electric energy supply system. It has to store enough energy for a 90 minute flight under OEI optimal conditions in order to comply with FAA and ICAO ETOPS90 regulations. The resulting battery size leads to a noticeable weight addition. A conventional two TF system therefore appeared to be the superior design solution in the early concept stages. But some additional considerations were taken into account. The U-Liner aims to position the TF system on the rear upper section of the aircraft in order to shield against fan, jet and turbine

noise. This would force the two TFs to be positioned within very close distance which is critical for safe operation. An uncontained disc failure e.g could severely damage the other TF and therefore be a single point of failure in the propulsion system [69]. In order for the two TF arrangement to offer appropriate system redundancy a protective casing would have to be incorporated to shield against these types of failures. But the location's long arm of lever causes a high weight sensitivity which imposes a major drawback of the two TF system.

The weight difference of the two arrangements is calculated in Table 5. The difference in battery weight results from the additional energy reserve the one TF system requires for an ETOPS 90 certification. The TF weights were calculated using empirical correlations taken from Raymer [55] and the weights of the casings are estimated based on material strength and density. Mission fuel weights were determined iteratively due to their dependency on SFC. Balancing all component weights including a growth factor [58] results in a 7937 kg weight penalty of the one TF System. This weight penalty has to be compensated by an improvement in TSFC. To calculate this required TSFC improvement which would represent a break even of the two systems, the specific air range can be used as a key figure of merit for vehicular performance [61, 64]. For a comparison of the two systems the aerodynamic performance L/D and the cruise velocity V_C are assumed to be the same. The only differences occur in fuel consumption $\Delta TSFC$ and in the systems integrated aircraft weight Δm_A.

Weight Item	Unit	Single TF	Two TFs
Battery	kg	17964	5914
Turbo Fans	kg	2600	4600
Casing	kg	400	1600
Mission Fuel	kg	20000	21350
Total	kg	40964	33464
Weight Difference	kg	7499	0
Growth Factor	kg	1.058	0
Weight Addition	kg	7937	0

Table 5: Comparison of Propulsion Systems

$$\Delta \frac{dR}{dW} = \frac{V_C}{\Delta TSFC} \cdot \frac{L}{D} \cdot \frac{1}{g \cdot \Delta m_A} = 0 \tag{5}$$

To achieve the same specific air range the one TF System has to compensate the 7937 kg weight penalty by improving its TSFC in cruise conditions by 5.8 % compared to the two TF system. This result is the baseline for finding an optimal TF arrangement that incorporates the NO_x reduction targets as well as noise levels and efficiency requirements.

6.4 Turbo Fan Cycle Optimization

To determine a TF technology that can achieve the required TSFC and NO_x reduction, a number of cycle performance optimizations were simulated in GasTurb12. Due to the support of the EFs, the TF can be sized for cruise instead of the usual top of climb conditions. The design point for all simulated cycles was therefore set to Ma 0.75 in ISA conditions at the initial cruise altitude. This cruise design point avoids oversizing and part load of the TF in cruise. It results in an increased combustor loading for the simulation and causes TF cycle temperatures to rise during cruise. Higher cycle temperatures of conventional TF cycles demand higher OPR levels to achieve optimal core efficiencies and reduce cruise TSFC [64]. The combination of high cycle temperatures and high OPRs however increases the engine's NO_x emission [64]. This trade off between TSFC and NO_x is known to be a general conflict of interest that limits the ability of conventional TF technology in achieving both efficiency improvements and emission reductions [64]. Hence a new core concept of the research program NEWAC [70] was down-selected from a number of promising TF technologies that were investigated as alternatives. It incorporates compressor intercooling and recuperation using heat exchanger technology. This advanced cycle technology referred to as intercooled recuperated aero engine (IRA) was assessed in a multi variable cycle optimization study to reduce TSFC and NO_x at the design point in cruise. Off-design performance and HPT material heat resistance were considered as constraints for TET and net thrust at take off. To illustrate part of this optimization, a parametric iteration of the key variables BPR and burner exit temperature is plotted in Fig 17.

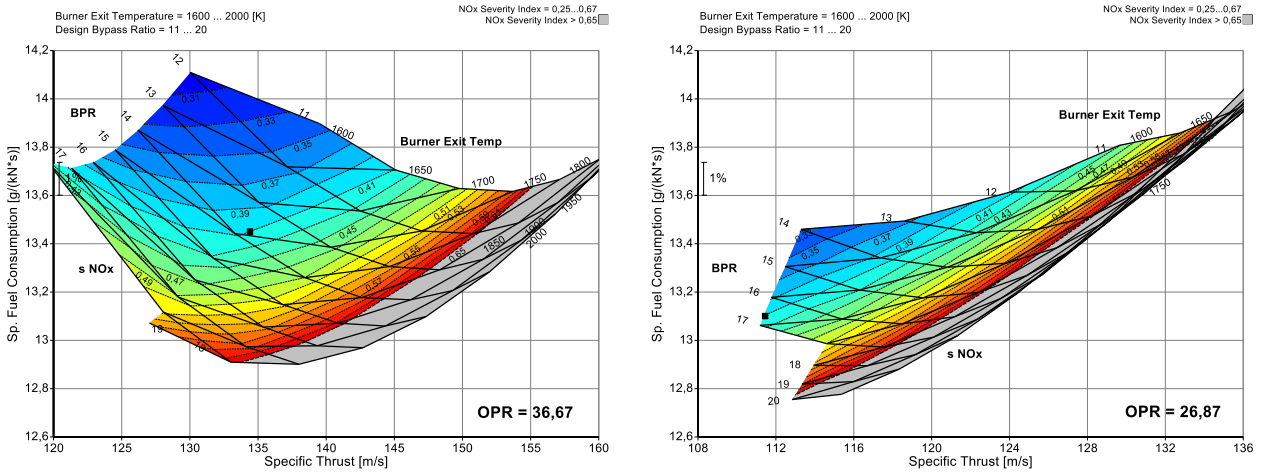

Figure 17: Parametric Optimization of IRA Cycle

The parametric plot on the left side of Fig 17 illustrates the trade off between TSFC and NO_x for an IRA cycle with an OPR of 36. The engine's NO_x severity parameter S_{NO_x} [71], illustrated by the colored zones, reaches a minimum in TSFC at one specific thrust level. Lowering the OPR to 26 (right plot) however, changes the general structure of the S_{NO_x} zones and allows to improve the engine's TSFC at the same S_{NO_x} value. The new optimum illustrated by the black dot, has a lower TSFC and a higher BPR without increasing the engines NO_x emission. The TET of the new optimum only differs by less then 1%. This could not be achieved with a conventional TF cycle which requires increased OPRs and TETs to improve efficiency levels at higher BPRs [64]. The IRA technology therefore offers great potential for reducing NO_x emissions and improving overall engine efficiency [70, 72].

Incorporating an IRA engine into the U-Liner concept yields some additional advantages for the heat exchanger technology. The IRA cycle largely benefits from the constant burner exit temperatures caused by the increased cruise loading condition. Conventional TETs in cruise are 300-400K below their corresponding take off values [72]. The optimal preliminary design point of the IRA cycle has a TET of 1733K during cruise and 1760K at take off in ISA+10 conditions. This flat temperature profile offers an ideal environment for the application of heat exchangers. The resulting improvement in cruise TSFC for a single large IRA engine is determined to be 15.3% compared to a system with two GTFs and 7.5% compared to a system with two smaller IRA engines (all with the same polytropic efficiencies). The efficiency gain of the single engine system therefore exceeds the required limit of 5.8%, causing it to be the superior propulsion system for the U-Liner concept. The IRA engine is also beneficial for reducing noise emissions. This is due to the smaller core diameters that in turn allow for higher BPRs at the same fan diameter.

6.5 Performance Comparison

To examen the U-Liner's NO_x emission, the LTO cycle conditions were simulated as off-design points for the IRA performance cycle. The reduction in total LTO NO_x emission is estimated to be 82% relative to a current generation Airbus A321. The corresponding characteristic value D_p/F_0 would be 78% below the CAEP 6 Limit. This already accounts for a drastic reduction of LTO NO_x emissions but it does not yet satisfy the design requirement. The reduction however represents an accurate estimation using a valid cycle design of a GasTurb optimization. To underline the impact of advanced cycle technology and hybrid propulsion a detailed comparison of LTO NO_x emission is given in table 6. The data for the A321's CFM56-5B2/P is taken from the ICAO Emission Database [73].

The GasTurb results presented in Table 6 are entirely based on a model for dual annular combustors and therefore do not account the effect of ultra low NO_x combustion technology such as RQL [71]. These new combustor types have tremendous potential to further reduce NO_x emissions but simulating their cycle performance requires the addition of empirical correlations for RQL combustors [74].

			A321		U-Liner	
ICAO Landing and Take Off Cycle			2x CFM56-5B2/P (2001)		1x IRA Engine (2035)	
Mode	Power [%]	Time [s]	Fuel Flow [kg/s]	EI_{NOx} [g/kg fuel]	Fuel Flow [kg/s]	EI_{NOx} [g/kg fuel]
Take Off	100	42	1.992	23.6	1.3633	17.22
Climb	85	132	1.598	19.6	1.0386	13.34
Approach	30	240	0.55	9.2	0	0
Taxi	7	1560	0.194	4	0	0
Aircraft LTO NO_x Emission [g]			15446		2814.84	
Reduction of LTO NO_x Emission					82%	

Table 6: LTO NO_x emission comparison

The resulting emission predictions should therefore be regarded as rough estimations.

To determine the effect of an RQL combustor an empirical correlation for RQL technology [74] was incorporated in the GasTurb performance simulation. The resulting LTO NO_x estimation yields a D_p/F_0 of 6.89 which is 87% below the CAEP 6 Limit and therefore exceeds the design target. A comparison of these results to current generation TFs based on the ICAO Emission Database is illustrated in Table 7 [73].

	A321 CFM56-5B2/P (2001)	A320 CFM56-5B6/P (2006)	A321 Neo PW 1133G-JM (2017)	U-Liner IRA + RQL Comb. (2035)
OPR	31.57	24.64	38.9	26.76
D_p/F_0	64.9	46.9	38.3	6.89
% below CAEP6 Limit	- 4.5%	8.8%	50.0%	87.3%

Table 7: Comparison of Characteristic Value

The CAEP Limits increase with higher OPRs which does not favor the IRA engine of the U-Liner. The low OPR however largely contributes to the reduction of cruise NO_x emission. For a comparison of cruise NO_x emission the CeRAS Reference Aircraft [66] is not entirely suitable due to its V2500 engine being older than 2005. To obtain a more accurate comparison a 2005 CFM56 was simulated in the same flight conditions as the IRA engine. The simulation determines the IRA cycle to have a 74% lower cruise NO_x emission on the 3200nm design mission. This is again a tremendous reduction but short of the design target. To achieve the required 80% reduction in cruise NO_x the U-Liner relies on the additional emission saving potential of alternative biofuels which have recently been identified to have a major impact on cruise emissions [75].

From an efficiency standpoint the U-Liner's propulsion system largely benefits from the single IRA engine's TSFC of just 13.09 g/kNs. This 20% improvement over the simulated CFM56 causes the U-Liner to consume 53% less fuel per 100 PAX km than a current generation Airbus A321. Compared to a larger Airbus A330-200 in a 300 PAX configuration the reduction in fuel consumption per 100 PAX km is beyond 60%.

7 Concept Feasibility

7.1 Weight Estimation

The weight estimation is based on a semi-empirical method taken from Torenbeek [10]. In order to compare the calculated system weights to current aircraft, the same method has been applied to both Airbus A321 and A330-200 as the U-Liner fills the size gap between these two. The primary target of lowering the structural weight is enhanced through the application of composite materials. In combination with technological advancements and making use of the material's anisotropy, weight

saving factors of 5-15% were assumed for different components with respect to the semi-empirical method.

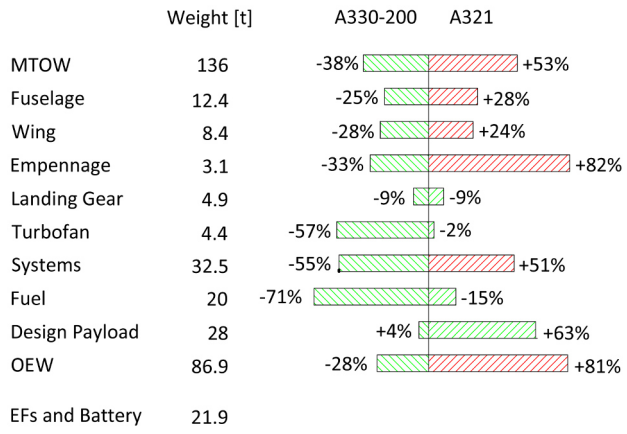

Figure 18: Weight Estimation and Comparison

For the fuselage, wing and empennage structures a 10% overall weight saving was presumed. The wing weight estimation is based on the FEM model, predicting a 8.4t structure. The wing position in conjunction with the rear engine mount also separates the landing gear from the wing structure, simultaneously making it shorter and thus lighter. This has been factored with a 15% weight reduction for the undercarriage. The structural savings for the single turbofan have been assumed with moderate 5% as these advancements mainly concern the engine casing. The batteries required for the hybrid configuration add a significant system weight due to the ETOPS certification. This however leads to substantial savings in fuel which directly influences the operational competitiveness of the U-Liner. Incorporating the battery weight into the OEW results in an overall reduction of 36% thereof compared to the A330-200 and a 61% increase compared to the A321. Furthermore the payload capability is superior to both baseline aircraft, underlining the usability as a short range freighter after decommission from passenger transport.

7.2 Cost Comparison

A primary goal resulting from the operational requirements is to reduce the Direct Operating Costs of the U-Liner. About 80% thereof are resembled by Cash Operating Costs (COC) [7], consisting of crew, maintenance, fee and fuel costs. An early estimation based on the method proposed by Thorbeck [76,77] is illustrated in Fig 19. These values were calculated for 1000 flight cycles assuming the same flight times for the U-Liner, Airbus A321 and A330-200. For comparison purposes, the costs are presented per passenger.

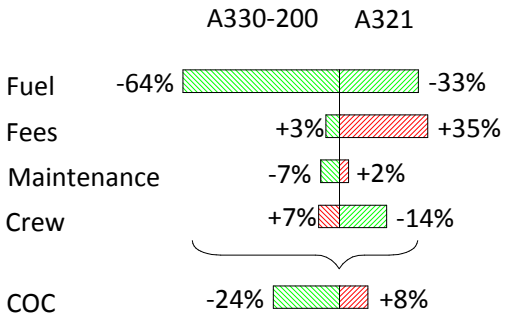

Figure 19: Per-Passenger Cost Comparison

In this comparison the A321 is the aircraft with the lowest fees for landing, ground handling and navigation since these are dependent on MTOW and payload. Maintenance costs scale with OEW and are highly dependent on the aero engine used. Due to the single turbofan configuration of the U-Liner the number of turbine stages is lowered to three for the entire aircraft which enables significant savings in maintenance costs. Furthermore, the fuel consumption per 100 PAX km is estimated to be 53% below an Airbus A321 for a 3200nm design mission. The aircraft comparison is based on a 2016 US airline fuel price of $0.34 Euro/liter$ [78]. The fuel costs are complemented by the electric energy required for the hybrid propulsion system which is predicted to be 10MWh for the entire design mission. As electricity prices vary greatly between different countries [79], the price was assumed to be $0.28 Euro/kWh$. Despite minor drops in fuel prices in recent years, the general trend is expected to continue upwards [3]. This supports the hybrid propulsion design for the U-Liner with the given entry into service horizon.

7.3 Sensitivity Analysis

The U-Liner's single TF design requires a large battery to provide enough energy in case of the single TF failing. One of the most critical variables therefore is the specific energy density of the battery system. To identify a minimum specific energy density the concept's sensitivity of this parameter is investigated. At a specific energy density of 1150 Wh/kg the single TF system has to deliver a 5.8% improved TSFC to compensate its the additional battery weight. The resulting minimum TSFC of 14.2 g/kNs is illustrated in Fig 20. This minimum however varies with the specific energy density. The black line in Fig 20 represents all combinations where the reduced TSFC of the single TF system exactly compensates its battery weight penalty and achieves the same specific range as a two TF system.

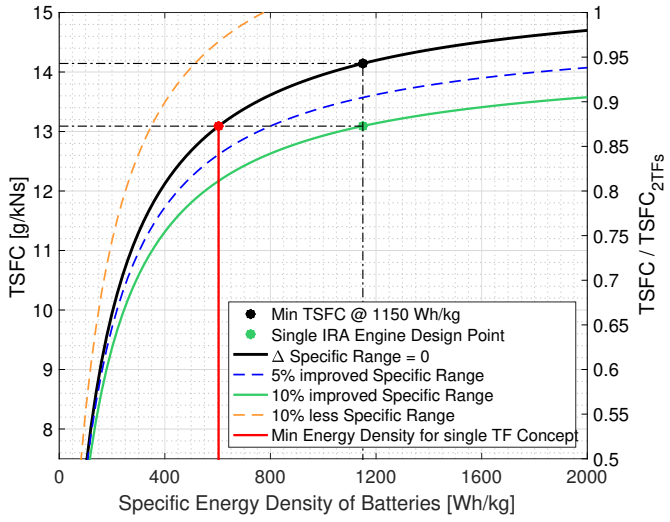

Figure 20: Sensitivity Analysis

The IRA engine however has an estimated TSFC of 13.09 g/kNs and therefore manages to improve the specific range by 10%. This is illustrated as the green line. For lower energy density this specific range improvement shrinks due to the increased battery weight. The advantage of the single IRA engine reaches zero at 600 Wh/kg. Every energy density below this minimum limit would cause the single IRA engine to achieve less specific range than a configuration with two GTFs and a smaller battery. The red line at 600 Wh/kg therefore represent the minimum energy density required for the single turbofan concept to be feasible.

8 Conclusion

The Urban Liner concept introduces a new aircraft configuration that incorporates and combines advantages of promising aerospace technologies to achieve the ambitious goals of DLR and NASA and deliver outstanding operational performance. To achieve the 42 dB noise reduction target the U-Liner introduces a single turbo fan hybrid design which is expected to reduce engine outlet velocities at take off by up to 60% compared to current configurations. The engines remaining jet stream, fan and turbine noises are shielded by the U-Liner's wide body and twin vertical tail system. This design is expected to significantly reduce sideline and flyover noise levels. It is combined with a morphing wing high lift system to reduce approach noise and achieve the cumulative noise reduction target.

The final airframe design has the noise shielding advantages of a BWB but avoids the economic drawbacks related to them. The U-Liner's advanced tube-and-wing configuration well cooperates with existing airport infrastructure and allows for future family concepts. It benefits from the introduction of advanced aerodynamics which achieve a significant reduction in the aircraft's overall drag. The reduced tail size as well as the application of hybrid laminar flow utilize the distributed electric fans during cruise and therefore represent additional measures for maximizing usability of hybrid propulsion.

The advanced aerodynamic technologies were integrated in a structural airframe design which was assessed and optimized using Finite Element Methods. The resulting layout not only takes advantage of carbon fibre materials for weight savings but incorporates their material properties to realize new design opportunities. The innovative split wing root design with its variable inlet geometry allows the integration of the electric fans and their combinational use to deliver propulsive support and reduce drag during cruise. This major feature of the U-Liner represents a new solution for compensating the

additional system weight of a hybrid aircraft. The support of the electric fans allow the turbo fan to be sized for cruise conditions instead of the usual top of climb conditions. This avoids oversizing of the turbo fan and by itself improves efficiency and emissions. It enables new turbo fan design opportunities and technologies.

The GasTurb cycle design optimization study that was based on the new cruise design point, identified the intercooled recuperated aero engine as the most promising turbo fan technology for the U-Liner's design targets. The heat exchanger hereby largely benefits from the steady loading conditions and the resulting flat temperature profile of the hybrid system. Combined with an ultra low NO_x combustor, the simulation of the intercooled recuperated aero engine estimates an 87% reduction of the LTO characteristic NO_x emission value relative to the CAEP 6 limit. Cruise NO_x emissions are estimated to be 74% lower compared to the simulated EIS 2005 CFM56 reference engine. With the addition of alternative biofuels a cruise NO_x reduction beyond 80% is expected.

With the advanced aerodynamic and propulsive technologies of the U-Liner cruise fuel consumption per PAX is estimated to be more than 50% lower relative to a current generation Airbus A321. Compared to a larger Airbus A330-200 in a 300 PAX configuration the reduction in fuel consumption per 100 PAX km is beyond 60%. These results lead to a very competitive market position of the U-Liner. To compare its operational capabilities a payload and range diagram is illustrated in Fig 21. It underlines the market positioning of the U-Liner. The aircraft offers a slightly larger maximum payload capacity than an Airbus A330-200 but only for a short range. For medium range missions the U-Liner offers superior payload and range capabilities to an Airbus A321.

At the design range of 3200nm the U-Liner manages a 50% increased payload relative to the A321, making it an ideal aircraft for high payload capacities on medium range missions. The application of a hybrid propulsion system also involves operational implications. The battery weight of the U-Liner varies with the requested ETOPS certification. This introduces additional flexibility for airline operations. A standard ETOPS 90 version is considered most profitable but a possible ETOPS 120 version would offer increased route flexibility and combined with a larger fuel capacity lends itself for longer flight operations. The specific battery energy density however limits the aircraft's ability for long haul applications. An ETOPS 180 certificate would require increased energy densities or an alternative two turbo fan configuration.

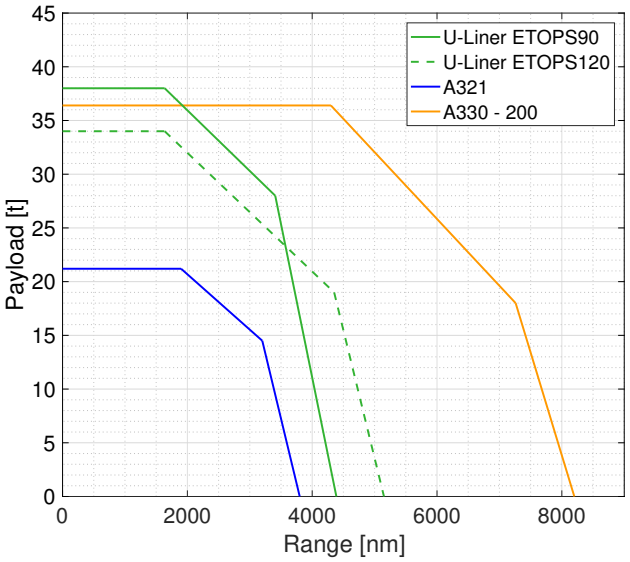

Figure 21: Payload Range Diagram

The U-Liner was developed as a pre-concept investigation study and encourages future research to further investigate its suggested technologies for noise and emission reduction. All noise predictions presented in the report are entirely based on comparisons and handbook methods. For a more accurate estimation of aircraft noise emissions a computational fluid dynamics model would be of great value. It would also allow a more detailed aerodynamic revision of the airframe and wing geometry. More accurate engine emission predictions are expected when incorporating future field testing data of low NO_x combustors into the engine's performance simulation.

References

[1] W. R. Graham, C. A. Hall, and M. Vera Morales, "The potential of future aircraft technology for noise and pollutant emissions reduction," *Transport Policy*, vol. 34, pp. 36–51, 2014.

[2] OAG, "Network of Air Travel Data," 2017. [Online]. Available: https://www.oag.com/

[3] Airbus S.A.S, "Global Market Forecast 2013-2032," Airbus, Tech. Rep., 2013.

[4] N. T. Birch, "2020 Vision: the Prospects for Large Civil Aircraft Propulsion," *Aeronautical Journal*, vol. 104, no. 1038, pp. 347–352, 2000.

[5] N. E. Antoine and I. M. Kroo, "Framework for Aircraft Conceptual Design and Environmental Performance Studies," *AIAA Journal*, vol. 43, no. 10, pp. 2100–2109, 2005.

[6] Boeing, "Current market outlook 2017-2036," 2017.

[7] M. Hornung, "Fundamentals of Aircraft Operations," 2016.

[8] Airbus, "Airbus Website," 2017. [Online]. Available: http://www.airbus.com/aircraft.html

[9] W. Dobrzynski, "Leiser Flugverkehr II – Abschlussveranstaltung Arbeitspaket 2B – Lärmarmer Zellenentwurf, V1," 2007, pp. 1–19.

[10] E. Torenbeek, *Advanced Aircraft Design.* John wiley & Sons Ltd., 2013.

[11] J. S. Gibson, "Non-engine Aerodynamic Noise Investigation of a Large Aircraft," *NASA Contractor Reports*, no. October, p. 55, 1974.

[12] R. H. Thomas, C. L. Burley, and E. D. Olson, "Hybrid Wing Body Aircraft System Noise Assessment with Propulsion Airframe Aeroacoustic Experiments," *International Journal of Aeroacoustics*, vol. 11, pp. 369–410, 2012.

[13] MIT, "NASA N+3 MIT Team Final Review," 2010. [Online]. Available: http://web.mit.edu/drela/Public/N+3/Final_slides.pdf

[14] T. A. Reist and D. W. Zingg, "The Lifting-Fuselage Aircraft Configuration," in *5th UTIAS International Workshop on Aviation and Climate Change*, Toronto, 2016.

[15] A. Abeysinghe, J. Whitmire, D. Nesthus, J. M. Goodrich, C. Vista, and G. Stuczynski, "QTD 2 (Quiet Technology Demonstrator 2) main landing gear noise reduction fairing design and analysis," *13th AIAA/CEAS Aeroacoustics Conference (28th AIAA Aeroacoustics Conference)*, vol. 2, pp. 1–18, 2007.

[16] W. Herkes, R. F. Olsen, and S. Uellenberg, "The Quiet Technology Demonstrator Program: Flight Validation of Airplane Noise-Reduction Concepts," *AIAA Paper 98-2611*, no. 2006-2720, pp. 8–10, 2006.

[17] H. Grieb, H. Schubert, *Projektierung von Turboflugtriebwerken.* Basel-Boston-Berlin: Birkhäuser Verlag, 2004.

[18] H. D. Kim, "Distributed Propulsion Vehicles," *27th International Congress of the Aeronautical Sciences*, pp. 1–11, 2010.

[19] H. D. Kim, G. V. Brown, and J. L. Felder, "Distributed Turboelectric Propulsion for Hybrid Wing Body Aircraft," in *2008 International Powered Lift Conference*, 2008, pp. 1–11.

[20] H. Martin, "Electric Flight - Potential and Limitations," *AVT-209 Workshop, Lisbon*, pp. 1–30, 2012.

[21] C. Thill, J. A. Etches, I. P. Bond, K. D. Potter, and P. M. Weaver, "Composite corrugated structures for morphing wing skin applications," *Smart Materials and Structures*, vol. 19, no. 12, p. 124009, 2010.

[22] L. Wiggins, M. Stubbs, C. Johnston, H. Robertshaw, C. Reinholtz, and D. Inman, "A Design and Analysis of a Morphing Hyper-Elliptic Cambered Span (HECS) Wing," *45th AIAA/ASME/ASCE/AHS/ASC Structures, Structural Dynamics & Materials Conference*, no. April, 2004.

[23] J. A. Hetrick, R. F. Osborn, S. Kota, P. M. Flick, and D. B. Paul, "Flight Testing of Mission Adaptive Compliant Wing," pp. 1–17, 2007.

[24] J. I. Hileman, Z. S. Spakovszky, M. Drela, M. A. Sargeant, and A. Jones, "Airframe Design for Silent Fuel-Efficient Aircraft," *Journal of Aircraft*, vol. 47, no. 3, pp. 956–969, 2010.

[25] T. Bauer and R. König, "Lärmminderung im Landeanflug durch Anpassung des Höhen- und Geschwindigkeitsprofils," pp. 1–14, 2016.

[26] O. I. Zaporozhets and V. I. Tokarev, "Aircraft noise modelling for environmental assessment around airports," *Applied Acoustics*, vol. 55, no. 2, pp. 99–127, 1998.

[27] K. Risse, "Preliminary Overall Aircraft Design with Hybrid Laminar Flow Control," Ph.D. dissertation, Rheinisch-Westfälischen Technischen Hochschule Aachen, 2016.

[28] D. V. M. R. H. Pettersen, "NASA Research On Viscous Drag Reduction," National Aeronautics and Space Administration, Tech. Rep., 1982.

[29] A. L. Braslow, *History of Suction-Type Laminar-Flow Control with Emphasis on Flight Resrearch:*, 1999, vol. 13.

[30] V.Schmitt, J. J. Thibert, and J. Reneaux, "ONERA Activities On Drag Reduction," Tech. Rep., 1990.

[31] A. Q. G. Redeker, K. H. Horstmann, H. Koester, "Investigations of high reynolds number laminar flow airfoils," *Journal of Aircraft*, vol. 25, no. 7, pp. 583–590, 1988.

[32] P. Arcara, D. Barlett, and L. McCullers, "Analysis for the Application of Hybrid LaminarFlow Control to a Long-Range Subsonic Transport Aircraft," Tech. Rep., 1991.

[33] J. Robert, "Hybrid Laminar Flow Control: A Challenge for a Manufacturer," in *First European Forum on Laminar Flow Technology.* DGLR-Bericht 92-06, 1992, pp. 294–308.

[34] J. Reneaux, "Overview on drag reduction technologies for civil transport aircraft," in *European Congress on Computational Methods in Applied Sciences and Engineering ECCOMAS*, no. July, 2004, pp. 1–18.

[35] M. Kruse, T. Wunderlich, and L. Heinrich, "A Conceptual Study of a Transonic NLF Transport Aircraft with Forward Swept Wings," in *30th AIAA Applied Aerodynamics Conference*, 2012, pp. 1–27. [Online]. Available: http://dx.doi.org/10.2514/6.2012-3208

[36] I. S. E. Din, J. L. Godard, A. M. Rodde, F. Moens, G. Andreutti, M. D. Muzio, R. Gemma, E. Baldassin, N. Calvi, I. S. E. Din, J. L. Godard, A. M. Rodde, F. Moens, G. Andreutti, and N. Laminar, "Natural Laminar Flow Transonic Wing Design Applied to Future Innovative Green Regional Aircraft," in *3AF / CEAS Conference "Greener Aviation: Clean Sky breakthroughs and worldwide status"*, no. Mar, Bruxelles, 2014.

[37] G. Hanks, G. Ledbetter, A. Moyer, and A. Nagel, "Hybrid Laminar Flow Control Study," BOEING Commercial Airplane Company, Tech. Rep., 1982.

[38] D. Scholz and S. Ciornei, "Mach number, relative thickness, sweep and lift coefficient of the wing - an empirical investigation of parameters and equations," in *Deutscher Luft- und Raumfahrtkongress*, 2005.

[39] C. Harris, "NASA Supercritical Airfoils," Tech. Rep., 1990.

[40] Robert J. Englar, "Overview of Circulation Control Pneumatic Aerodynamics: Blown Force and Moment Augmentation and Modification as Applied Primarily to Fixed Wing Aircraft," in *Proceedings of the 2004 NASA / ONR Circulation Control Workshop*, 2004.

[41] Robert J. Englar, Marilyn J. Smith, Sean M. Kelley, and Richard C. Rover III, "Development of Circulation Control Technology for Application to Advanced Subsonic Transport Aircraft, Part I," *AIAA Journal of Aircraft*, vol. 31, no. 5, pp. 1169–1177, 1994.

[42] Robert J. Englar, Marilyn J. Smith, Sean M. Kelley, and Richard C. Rover III, "Development of Circulation Control Technology for Application to Advanced Subsonic Transport Aircraft, Part II," *AIAA Journal of Aircraft*, vol. 31, no. 5, pp. 1169–1177, 1994.

[43] R. D. Joslin, "Overview of Laminar Flow Control," 1998.

[44] H. Heyson, G. Riebe, and C. Fulton, "Theoretical Parametric Study of the Relative Advantages of Winglets and Wing-Tip Extensions," Tech. Rep., 1977.

[45] Ph. Poisson-Quinton, "Aircraft Drag Prediction and Reduction," Tech. Rep., 1985.

[46] M. Drela, "Development of the D8 Transport Configuration," in *29th AIAA Applied Aerodynamics Conference*, no. June, Honolulu, 2011.

[47] "Metro Aerospace," 2017. [Online]. Available: http://www.metroaerospace.com/

[48] G. Warwick, "Drag-Reducing Microvanes Make It To The C-130 Hercules Fleet," *Aviation Week and Space Tehcnology*, no. May 30., 2017.

[49] O. Cazals and J. G. de la Sagne, "Airplane with flat rear fuselage said queue-de-morue empennage," 2010.

[50] V. Schmitt, J. P. Archambaud, K. H. Horstmann, and A.Quast, "Hybrid Laminar Fin Investigation," in *RTO A VT Symposium on "Active Control Technology for Enhanced Performance Operational Capabilities of Military Aircraft, Land Vehicles and Sea Vehicles"*, Braunschweig, 2000.

[51] K. Stadlberger and M. Hornung, "Challenges in the modelling of blown circulation control aerofoils," in *Deutscher Luft- und Raumfahrtkongress*, 2014, pp. 1–13.

[52] M. H. Sadraey, *Aircraft Design: a system engineering approach*. Wiley, 2013.

[53] J. J. Rising, "Development of a Reduced Area Horizontal Tail for a Wide Body Jet Aircraft," NASA, Tech. Rep., 1984.

[54] G. van Es, "Rapid Estimation of the Zero-Lift Drag Coefficient of Transport Aircraft," *Journal of Aircraft*, vol. 93, no. August, pp. 597–599, 2002.

[55] D. P. Raymer, *Aircraft Design A Conceptual Approach*. American Institute of Aeronautics and Astronautics, 1992.

[56] N. Paletta, M. Belardo, and M. Pecora, "Load Alleviation on a Joined-Wing Unmanned Aircraft," *Journal of Aircraft*, vol. 47, no. 6, pp. 2005–2016, 2010.

[57] T. Buhl, D. C. Bak, M. Gaunaa, P. B. Andersen, and C. Bak, "Load alleviation through adaptive trailing edge control surfaces: ADAPWING overview," *European Wind Energy Conference*, pp. 1–8, 2006.

[58] M. Hornung, "Flugzeugentwurf," 2016.

[59] K. G. Pratt, "A Survey of Active Controls Benefits to Superonic Transports," 1974.

[60] H. Kuhn, A. Seitz, L. Lorenz, A. Isikveren, and A. Sizmann, "Progress and perspectives of electric air transport," *28th Congress of the International Council of the Aeronautical Sciences 2012, ICAS 2012*, vol. 6, pp. 4886–4899, 2012.

[61] A. Seitz, O. Schmitz, A. T. Isikveren, and M. Hornung, "Electrically Powered Propulsion: Comparison and Contrast to Gas Turbines," *Deutscher Luft- und Raumfahrtkongress 2012*, no. April 2015, pp. 1–14, 2012.

[62] H. Kuhn and A. Sizmann, "Fundamental Prerequisites for Electric Flying," in *Deutscher Luft- und Raumfahrtkongress 2012*, 2012, pp. 1–8.

[63] M. Hornung, A. T. Isikveren, M. Cole, and A. Sizmann, "Ce-Liner - Case Study for eMobility in Air Transportation," *2013 Aviation Technology, Integration, and Operations Conference*, no. April 2015, 2013.

[64] H. Rick, *Gasturbinen und Flugantriebe Grundlagen, Betreibsverhalten und Simulation.* Springer Verlag, 2013.

[65] C. A. Luongo, P. J. Masson, T. Nam, D. Mavris, H. D. Kim, G. V. Brown, M. Waters, and D. W. Hall, "Next Generation More-Electric-Aircraft: A Potential Application for HTS Superconductors," *Applied Superconductivity*, vol. 19, no. 3, pp. 1055–1068, 2009.

[66] RWTH Aachen, "CeRAS Reference Aircraft Database," Tech. Rep., 2017. [Online]. Available: http://ceras.ilr.rwth-aachen.de/trac

[67] M. W. Scott, "Aircraft Design Considerations to Meet One Engine Inoperative (OEI) Safety Requirements," no. August, 2012.

[68] A. Seitz, A. T. Isikveren, and M. Hornung, "Pre-Concept Performance Investigation of Electrically Powered Aero-Propulsion Systems," *49th AIAA/ASME/SAE/ASEE Joint Propulsion Conference*, 2013.

[69] M. C. Schwarze and T. Zold, "Angepasste Flugzeugkonfigurationen Für Die Energieeffiziente Open-Rotor Integration Auf Zukünftigen Kurzstrecken-Verkehrsflugzeugen," in *Deutscher Luft- und Raumfahrtkongress*, 2013, pp. 1–19.

[70] G. Wilfert, J. Sieber, A. Rolt, N. Baker, A. Touyeras, and S. Colantuoni, "New Environmental Friendly Aero Engine Core Concepts," *18th International Symposium on Air Breathing Engines*, pp. 1–11, 2007.

[71] N. R. C. Comittee of Aeronautical Technology, *Aeronautical Technology for the Twenty-First Century.* Washington: National Acady Press, 1992.

[72] S. Boggia and K. Rud, "Intercooled recuperated gas turbine engine concept," in *41st AIAA/ASME/SAE/ASEE Joint Propulsion Conference & Exhibit*, no. July, 2005, pp. 1–11.

[73] ICAO, "Emission Database," 2017. [Online]. Available: https://www.easa.europa.eu/document-library/icao-aircraft-engine-emissions-databank

[74] K. G. Kyprianidis, D. Nalianda, and E. Dahlquist, "A NOx Emissions Correlation for Modern RQL Combustors," *Energy Procedia*, vol. 75, no. March 2017, pp. 2323–2330, 2015.

[75] R. H. Moore, K. L. Thornhill, B. Weinzierl, D. Sauer, E. D'Ascoli, J. Kim, M. Lichtenstern, M. Scheibe, B. Beaton, A. J. Beyersdorf, J. Barrick, D. Bulzan, C. A. Corr, E. Crosbie, T. Jurkat, R. Martin, D. Riddick, M. Shook, G. Slover, C. Voigt, R. White, E. Winstead, R. Yasky, L. D. Ziemba, A. Brown, H. Schlager, and B. E. Anderson, "Biofuel blending reduces particle emissions from aircraft engines at cruise conditions," *Nature*, vol. 543, no. 7645, pp. 411–415, 2017.

[76] J. P. D. I. Thorbeck, "Flugzeugentwurf," 2014.

[77] K. Franz, "CeRAS Direct Operating Cost (DOC) Model," 2014. [Online]. Available: http://ceras.ilr.rwth-aachen.de/trac/wiki/CeRAS/ToolsAndMethodologies/DOC

[78] Statista, "U.S. airline fuel cost from 2004 to 2016." [Online]. Available: https://www.statista.com/statistics/197689/us-airline-fuel-cost-since-2004/

[79] Statista, "Average electricity prices globally in 2015 by select country," 2017. [Online]. Available: https://www.statista.com/statistics/477995/global-prices-of-electricity-by-select-country/

Student Contact

Christian Decher
Amalienstraße 45
80799 München
Deutschland

Daniel Metzler
Freisinger Landstr. 45a
85748 Garching bei München
Deutschland

Soma Varga
Schlößlanger 7
80939 München
Deutschland